

## BIFURCATIONS OF PATTERNED SOLUTIONS IN THE DIFFUSIVE LENGYEL-EPSTEIN SYSTEM OF CIMA CHEMICAL REACTIONS

JIAYIN JIN, JUNPING SHI, JUNJIE WEI AND FENGQI YI

**ABSTRACT.** Bifurcations of spatially nonhomogeneous periodic solutions and steady state solutions are rigorously proved for a reaction-diffusion system modeling CIMA chemical reaction. The existence of these patterned solutions shows the richness of the spatiotemporal dynamics including Turing instability and oscillatory behavior. Examples of numerical simulation are also shown to support and strengthen the analytical approach.

**1. Introduction.** In 1744, Abraham Trembley published a book entitled *Mémoires, Pour Servir à l'Histoire d'un Genre de Polypes d'Eau Douce, à Bras en Forme de Cornes* (Memoirs concerning the natural history of a type of freshwater polyp with arms shaped like horns) [10, 19], which contained the first scientific study of the regeneration and pattern formation of *hydra*, the freshwater polyp. In order to model this interesting and important phenomenon in biological pattern formation, in his seminal paper [20], Turing showed mathematically that a system of coupled reaction-diffusion equations could give rise to spatial concentration patterns of a fixed characteristic length from an arbitrary

---

2010 AMS *Mathematics subject classification.* Primary 35K57, 35B32, 37G15, 35B10, 92E20, 80A32, 92B05.

*Keywords and phrases.* Lengyel-Epstein chemical reaction, reaction-diffusion system, Hopf bifurcation, steady state bifurcation, spatially non-homogeneous periodic orbits, global bifurcation.

The second, third and fourth authors were supported by the National Natural Science Foundation of China (Nos. 10671049, 10771045, 11001063 and 10926148, respectively). The second author was supported by the Longjiang Professorship of Department of Education of Heilongjiang Province, National Science Foundation of U.S. and Summer Research Grant of College of William and Mary. The third author was supported by Specialized Research Funds for the Doctoral Program of Higher Education. The fourth author was supported by the China Postdoctoral Science Foundation (20100471266), Science Council of Heilongjiang Province (A200806), Fundamental Research Funds for the Central Universities (HEUCF20101106), and by the Fundamental Research Foundation of Harbin Engineering University (HEUFT08033).

The fourth author is the corresponding author.

Received by the editors on June 16, 2010, and in revised form on February 9, 2011.

DOI:10.1216/RMJ-2013-43-5-1637 Copyright ©2013 Rocky Mountain Mathematics Consortium

initial configuration due to the so-called *diffusion-driven instability*, that is, diffusion could destabilize an otherwise stable equilibrium of the reaction-diffusion system and lead to nonuniform spatial patterns.

Over the years, Turing's idea has attracted the attention of a great number of investigators and was successfully developed on the theoretical background. Not only it has been studied in biological and chemical fields, some investigations range as far as economics, semiconductor physics and star formation (see [2, 3, 12]). However, the research for Turing patterns in real chemical or biological systems turned out to be difficult.

The first experimental observation of a Turing pattern in a chemical reactor was due to De Kepper's group, who observed a spotty pattern in a chlorite-iodide-malonic acid (CIMA) reaction [1] in 1990. The experiment on the CIMA reaction has revealed the existence of stationary space periodic concentration patterns, the so-called Turing structures, in open gel reactors. Later, Lengyel and Epstein suggested [8] that these patterns could arise because the iodine activator species forms a reversible complex of low mobility with the starch molecules used as color indicator for this reaction. In particular, they have also developed [9] a simple two-variable model that includes the three overall stoichiometric processes that lie at the heart of the mechanism of the CIMA reaction: the chlorine dioxide-iodine-malonic acid model. The corresponding dimensionless reaction-diffusion equations allowing for complex formation take the form:

$$(1.1) \quad \begin{cases} u_t = \Delta u + a - u - \frac{4uv}{1+u^2} & x \in \Omega, t > 0, \\ v_t = \sigma \left[ c\Delta v + b\left(u - \frac{uv}{1+u^2}\right) \right] & x \in \Omega, t > 0, \\ u(x, 0) = u_0(x), v(x, 0) = v_0(x) & x \in \Omega, \\ \partial_\nu u = \partial_\nu v = 0 & x \in \partial\Omega, t > 0, \end{cases}$$

where  $\Omega$  is a bounded connected domain (the reactor) in  $\mathbf{R}^n$ , ( $n \geq 1$ ), with smooth boundary  $\partial\Omega$ . The reactor is assumed to be closed; thus, reflexive Neumann boundary condition is imposed (here  $\partial_\nu u$  is the outer normal derivative of  $u$ );  $u(x, t)$  and  $v(x, t)$  denote the dimensionless iodide ( $I^-$ ) and chlorite ( $ClO_2^-$ ) concentrations, respectively,  $a$  and  $b$  are parameters related to the feed concentrations,  $c$  is the ratio of the diffusion coefficients and  $\sigma > 1$  is a rescaling parameter depending on the concentration of the starch, which enlarges the effective diffusion ratio to  $\sigma c$ .

The experimental observation of Turing patterns renewed the interest in these complex systems, and subsequently, a lot of research has been carried out employing theoretical investigations, including several rigorous mathematical treatments [6, 7, 13, 17, 21, 24, 25].

In [13], Ni and Tang considered both existence and nonexistence for the steady states of the system. They showed that, roughly speaking, if parameter  $a$  (related to the feed concentrations), the size of the reactor  $\Omega$  (reflected by its first eigenvalue), or the “effective” diffusion rate  $d = c/b$  is not large enough, then the system has no nonconstant steady states. On the other hand, if parameter  $a$  lies in a suitable range, then the system possesses nonconstant steady states for large  $d$ . These results further verify the original idea in “diffusion-driven instability” of Turing. Jang, Ni and Tang [6] further considered the global bifurcation structure of the set of nonconstant steady states in the one-dimensional case and clarified the limiting behavior of the steady states by using a shadow system approach.

In [24], the authors gave a detailed Hopf bifurcation analysis for both the ODE and PDE models, deriving a formula for determining the direction of the Hopf bifurcation and the stability of the bifurcating spatially homogeneous periodic solutions. On the other hand, in [25], the authors considered the global asymptotical behavior of solutions of the system, and they identified a parameter range in which the constant steady state is globally asymptotically stable; they also showed that, for small spatial domains and not so small  $a$ , all solutions eventually converge to some spatially homogeneous and time-periodic solution when the constant steady state is locally unstable. These results provided another step towards the complete understanding of the asymptotical dynamics of the diffusive Lengyel-Epstein system (1.1).

Although Turing instability results in spatiotemporal patterns that are stationary in time, the diffusive Lengyel-Epstein system can also exhibit a variety of complex spatiotemporal phenomena. Our main contribution in this article is a bifurcation analysis from the constant steady state solution when the spatial domain  $\Omega$  is one-dimensional. But, instead of using the effective diffusion rate  $d$  as bifurcation parameter (see [6, 13]), we use the feeding rate  $a$  of iodide (or equivalently  $\alpha = a/5$ ) as the bifurcation parameter. Our main results are proved for the case that the constant steady state is not stable even with respect to ODE dynamics (recall the Turing instability region is when the

system is stable with respect to the ODE but unstable for PDE). We rigorously prove that, in this parameter range, the system undergoes a sequence of bifurcations generating spatially nonhomogeneous steady state solutions and also spatially nonhomogeneous time-periodic solutions. This strongly suggests the richness of spatiotemporal patterns for these parameters.

In a survey paper, Maini et al. [11] stated that, *Exploration of a more detailed RD model of the CIMA reaction may therefore reveal behaviour not previously reported in the reaction. Examples include the Turing-Hopf (or spatial-Hopf) bifurcation in which the resulting spatial patterns oscillate in both space and time, the interaction of Turing-Hopf and Turing-type patterns, and the interaction of two Turing-type patterns.* Here our results exactly answer the question about spatial pattern oscillation in both space and time. We find parameter ranges for spatial Hopf bifurcations, and numerical simulation in these ranges suggests the existence of stable patterns oscillate in both space and time (see Figure 4.5.)

Our results are robust as the parameter range covers almost all  $a > 0$ , and the effective diffusion rate  $d$  does not have to be small or large as in Turing bifurcation (see Theorems 2.1 and 3.2 for the precise statement). On the other hand, our result can also recover the well-known Turing bifurcation as in [6]. We also remark that the existence of spatially nonhomogeneous periodic solutions for such an autonomous reaction-diffusion system is rarely shown in the literature, and here we follow an approach initiated in [26], in which a diffusive predator-prey system was studied. These spatially nonhomogeneous periodic solutions are not driven by a periodic force or a delay effect; hence, they are diffusion driven periodic solutions. We use Hopf bifurcation theory to prove the existence of these solutions. Hence, the existence is essentially local (near the bifurcation points). Although there is an abstract theory of global bifurcation for the periodic orbits [22, 23], not much information is shown by the global theorem as there is little knowledge on the period of these solutions. But our results are useful for future numerical detection of branches of periodic orbits. Stability of the periodic orbits is also not known except near the bifurcation points.

Our results also complement earlier results in [6, 13] in a few ways. It was shown in [13] that, if  $d$  is small, then the system has no nonconstant steady states. Our results imply that, when  $d$  is small, the system could

still have many periodic solutions; hence, the system likely tends to some periodic patterns instead of stationary ones (see Theorem 2.1). Our results also suggest a rather complete bifurcation diagram with parameter  $a$ : when  $a$  is small, the constant steady state is globally asymptotically stable from [25]; then, when  $a$  increases, the constant steady state loses stability either to a non-constant steady state via a Turing bifurcation, or loses stability to a periodic solution via Hopf bifurcation. A more precise and complete discussion on the bifurcation diagram can be found in the concluding remarks in Section 5.

Some numerical simulations with appropriate parameters are included in Section 4. These parameters are chosen motivated by the analytical bifurcation analysis. Solutions can be seen to converge to constant steady state and periodic solutions, or spatial dependent steady state and periodic solutions, and these results agree nicely with what our bifurcation analysis suggests. Numerical simulations also hint that the full dynamics is still more complicated than what has been found analytically. Further numerical and analytical investigation are still desired for a complete understanding of the spatiotemporal dynamics. Analysis of two spatial dimension domain problems and careful comparison to the patterns in the original Lengyel-Epstein system or CIMA reaction experiment remain interesting open questions.

The remaining part of the paper is organized as follows. In Section 2, we perform Hopf bifurcation analysis of the system. In Section 3, steady state bifurcations and the interaction between Hopf and steady state bifurcations are studied. Several examples with particular parameters are discussed in Section 4, and numerical simulations are shown to complement the analytical results. Concluding remarks are in Section 5. Two general bifurcation theorems, Hopf bifurcation and steady state bifurcation theorems, on the general reaction-diffusion system are given in the Appendix, for the sake of completeness. Throughout the paper, we always let  $\mathbf{N}$  denote the set of all the positive integers, and  $\mathbf{N}_0 = \mathbf{N} \cup \{0\}$ .

**2. Hopf bifurcation analysis.** In this section, we consider the Hopf bifurcation for the diffusive Lengyel-Epstein model subject to Neumann boundary conditions on the spatial domain  $\Omega = (0, \ell\pi)$ , with  $\ell \in \mathbf{R}^+$ , by applying some general results on bifurcation (which are summarized

in the Appendix). We introduce new parameters

$$d = \frac{c}{b}, \quad m = \sigma b, \quad \alpha = \frac{a}{5},$$

so system (1.1) is now in the following form:

$$(2.1) \quad \begin{cases} u_t = u_{xx} + 5\alpha - u - \frac{4uv}{1+u^2} & x \in (0, \ell\pi), t > 0, \\ v_t = m \left( dv_{xx} + u - \frac{uv}{1+u^2} \right) & x \in (0, \ell\pi), t > 0, \\ u_x(x, t) = v_x(x, t) = 0 & x = 0, \ell\pi, t > 0, \\ u(x, 0) = u_0(x), v(x, 0) = v_0(x) & x \in (0, \ell\pi). \end{cases}$$

In the following, we shall work with the new parameters  $\alpha$ ,  $m$  and  $d$  instead of the original four parameters  $\alpha$ ,  $\sigma$ ,  $b$  and  $c$ . Note that  $d$  is the effective diffusion coefficient used in [13] and  $m$  and  $\alpha$  are two essential parameters for the ODE system (see the bifurcation diagram in [24]). System (2.1) has one unique positive constant steady state solution  $(\alpha, 1 + \alpha^2) := (u_\alpha, v_\alpha)$ . In the following, we choose the fixed parameters  $d$ ,  $m$  and  $\ell$  properly and use  $\alpha$  as the main bifurcation parameter.

We define

$$X := \{ (u, v) \in H^2[(0, \ell\pi)] \times H^2[(0, \ell\pi)] \mid u'(0) = v'(0) = u'(\ell\pi) = v'(\ell\pi) = 0 \}.$$

The linearized operator of system (2.1) evaluated at  $(\alpha, 1 + \alpha^2)$  is

$$L(\alpha) := \begin{pmatrix} \frac{\partial^2}{\partial x^2} + \frac{3\alpha^2 - 5}{1 + \alpha^2} & -\frac{4\alpha}{1 + \alpha^2} \\ \frac{2m\alpha^2}{1 + \alpha^2} & md \frac{\partial^2}{\partial x^2} - \frac{m\alpha}{1 + \alpha^2} \end{pmatrix}.$$

It is well known that the eigenvalue problem

$$-\psi'' = \mu\psi, \quad x \in (0, \ell\pi), \quad \psi'(0) = \psi'(\ell\pi) = 0,$$

has eigenvalues  $\mu_n = n^2/\ell^2$  ( $n = 0, 1, 2, \dots$ ), with corresponding eigenfunctions  $\psi_n(x) = \cos(n/\ell)x$ . Let

$$\begin{pmatrix} \phi \\ \varphi \end{pmatrix} = \sum_{n=0}^{\infty} \begin{pmatrix} a_n \\ b_n \end{pmatrix} \cos \frac{n}{\ell} x$$

be an eigenfunction for  $L(\alpha)$  with eigenvalue  $\mu(\alpha)$ , that is,  $L(\alpha)(\phi, \varphi)^T = \mu(\alpha)(\phi, \varphi)^T$ . Then it is easy to show (see [26]) that, for any  $n \in \mathbf{N}_0$ , such that  $L_n(\alpha)(a_n, b_n)^T = \mu(\alpha)(a_n, b_n)^T$ , where  $L_n$  is defined as

$$L_n(\alpha) := \begin{pmatrix} -\frac{n^2}{\ell^2} + \frac{3\alpha^2 - 5}{1 + \alpha^2} & -\frac{4\alpha}{1 + \alpha^2} \\ \frac{2m\alpha^2}{1 + \alpha^2} & -md\frac{n^2}{\ell^2} - \frac{m\alpha}{1 + \alpha^2} \end{pmatrix}, \quad n = 0, 1, 2, \dots,$$

the characteristic equation of  $L_n(\alpha)$  is

$$\mu^2 - \mu T_n + D_n = 0, \quad n = 0, 1, 2, \dots,$$

where

$$(2.2) \quad \begin{aligned} T_n(\alpha) &:= \frac{3\alpha^2 - 5 - m\alpha}{1 + \alpha^2} - \frac{n^2}{\ell^2}(1 + md), \\ D_n(\alpha) &:= m \left[ \frac{5\alpha}{1 + \alpha^2} - \frac{n^2}{\ell^2} \left( \frac{d(3\alpha^2 - 5) - \alpha}{1 + \alpha^2} \right) + \frac{n^4}{\ell^4} d \right], \end{aligned}$$

and the eigenvalues  $\mu(\alpha)$  of  $L_n(\alpha)$  are given by

$$\mu(\alpha) = \frac{T_n(\alpha) \pm \sqrt{T_n^2(\alpha) - 4D_n(\alpha)}}{2}, \quad n = 0, 1, 2, \dots$$

We identify the Hopf bifurcation value  $\alpha$  satisfying the condition for Hopf bifurcation, which takes the following form (see Appendix, or [26] for details):

( $H_1$ ) There exists an  $n \in \mathbf{N}_0$ , such that

$$T_n(\alpha) = 0, \quad D_n(\alpha) > 0; \quad T_j(\alpha) \neq 0, \quad D_j(\alpha) \neq 0 \quad \text{for } j \neq n;$$

and let the unique pair of complex eigenvalues near the imaginary axis be  $\gamma(\alpha) \pm i\omega(\alpha)$ . Then the following transversality condition holds:

$$(2.3) \quad \gamma'(\alpha) \neq 0.$$

We rewrite  $T_n(\alpha)$  as  $T_n(\alpha) = A(\alpha) - p(1 + md)$ , where  $p = n^2/\ell^2$  and

$$A(\alpha) = \frac{3\alpha^2 - m\alpha - 5}{1 + \alpha^2}.$$

Solving  $p$  from  $T_n(\alpha) = 0$ , we have

$$(2.4) \quad p = \frac{1}{1 + md} A(\alpha).$$

It follows by direct calculation that

$$A'(\alpha) = \frac{m\alpha^2 + 16\alpha - m}{(1 + \alpha^2)^2} \begin{cases} > 0 & \text{if } \alpha > \alpha^*, \\ = 0 & \text{if } \alpha = \alpha^*, \\ < 0 & \text{if } 0 < \alpha < \alpha^*, \end{cases}$$

where  $\alpha^* = (-8 + \sqrt{64 + m^2})/m$ . Obviously,  $0 < \alpha^* < 1$ . A straightforward analysis shows that  $A(\alpha)$  achieves its minimal value  $A(\alpha^*) = -(3\alpha^4 + 8\alpha^2 + 5)/(1 - \alpha^4)|_{\alpha=\alpha^*} < 0$  at  $\alpha = \alpha^*$ , and  $\sup_{\alpha>0} A(\alpha) = \lim_{\alpha \rightarrow \infty} A(\alpha) = 3 > 0$ . Then there exists a unique point  $\alpha_0$ , with  $\alpha^* < 1 < \alpha_0 := (m + \sqrt{m^2 + 60})/6$  such that  $A(\alpha_0) = 0$ . In particular,  $A(\alpha) > 0$  and  $A(\alpha)$  is strictly increasing in  $(\alpha_0, \infty)$ .

Define

$$\ell_n = n\sqrt{\frac{1 + md}{3}}, \quad n = 0, 1, 2, \dots$$

Then, for  $\ell_n < \ell \leq \ell_{n+1}$  and  $0 \leq j \leq n$ , we define  $\alpha_j^H$  to be the solution of (2.4) satisfying  $0 < \alpha_0 \leq \alpha_j^H < +\infty$ . In fact, if we define

$$\alpha_1(\tilde{p}) = \frac{m + \sqrt{m^2 + 4(3 - \tilde{p})(5 + \tilde{p})}}{2(3 - \tilde{p})},$$

then  $\alpha_j^H = \alpha_1((1 + md)j^2/\ell^2)$  from (2.4). These points satisfy

$$0 < \alpha^* < \alpha_0^H (= \alpha_0) < \alpha_1^H < \dots < \alpha_n^H < +\infty.$$

Clearly,  $T_j(\alpha_j^H) = 0$  and  $T_i(\alpha_j^H) \neq 0$  for  $i \neq j$ . Now we only need to verify whether  $D_i(\alpha_j^H) \neq 0$  for all  $i \in \mathbf{N}_0$  and, in particular,  $D_j(\alpha_j^H) > 0$ .

Here we will derive a set of conditions on the parameters so that  $D_i(\alpha_j^H) > 0$ , for each  $i = 0, 1, 2, \dots$ . Then we have the following main result in this section:



**Theorem 2.1.** *For any  $n \in \mathbf{N}$ ,  $m > 0$ , if*

$$(2.5) \quad \ell > \sqrt{2n}/\sqrt{3},$$

*then there exists a  $d_* = d_*(m, \ell, n) > 0$  such that, when  $0 < d < d_*$ , there exist  $n + 1$  points  $\alpha_j^H = \alpha_j^H(d, m, \ell)$ ,  $0 \leq j \leq n$ , satisfying*

$$0 < \alpha_0^H < \alpha_1^H < \alpha_2^H < \dots < \alpha_n^H < \infty.$$

*At each  $\alpha = \alpha_j^H$ , system (2.1) undergoes a Hopf bifurcation, and the bifurcating periodic solutions near  $(\alpha, u, v) = (\alpha_j^H, \alpha_j^H, 1 + (\alpha_j^H)^2)$  can be parameterized as  $(\alpha(s), u(s), v(s))$  so that  $\alpha(s) \in C^\infty$  in the form of  $\alpha(s) = \alpha_j^H + o(s)$  for  $s \in (0, \delta)$  for some small  $\delta > 0$ , and,*

$$\begin{cases} u(s)(x, t) = \alpha_j^+ s(a_n e^{2\pi it/T(s)} + \overline{a_n} e^{-2\pi it/T(s)}) \cos \frac{n}{\ell} x + o(s), \\ v(s)(x, t) = 1 + (\alpha_j^H)^2 + s(b_n e^{2\pi it/T(s)} + \overline{b_n} e^{-2\pi it/T(s)}) \cos \frac{n}{\ell} x + o(s), \end{cases}$$

*where  $(a_n, b_n)$  is the corresponding eigenvector, and  $T(s) = 2\pi\sqrt{D_j(\alpha_j^H)} + o(s)$  ( $D_j$  is defined in (2.2)). Moreover,*

1. *The bifurcating periodic solutions from  $\alpha = \alpha_0^H$  are spatially homogeneous, which coincide with the periodic solutions of the corresponding ODE system;*
2. *The bifurcating periodic solutions from  $\alpha = \alpha_j^H$  are spatially nonhomogeneous.*

*Proof.* We assume that  $0 < d < m^{-1}$ , and hence  $0 < md < 1$ . We define  $p_j := j^2/\ell^2$ . Since  $\ell$  satisfies (2.5), then  $\ell > \tilde{\ell}_n$  under the assumption  $md < 1$ , and  $\alpha_j^H$  ( $j = 0, 1, 2, \dots, n$ ) are well-defined. First it is clear that

$$\frac{d[3(\alpha_j^H)^2 - 5] - \alpha_j^H}{1 + (\alpha_j^H)^2} < 3d.$$

On the other hand,

$$\frac{3(\alpha_j^H)^2 - 5 - m\alpha_j^H}{1 + (\alpha_j^H)^2} = (1 + md)p_j \leq (1 + md)p_n;$$

hence, from  $md < 1$ ,

$$\alpha_j^H < \frac{m + \sqrt{m^2 + 64}}{2(3 - (1 + md)p_n)} < \frac{m + \sqrt{m^2 + 64}}{2(3 - 2p_n)}.$$

Also,  $\alpha_j^H \geq \alpha_0^H > 1$ . Then

$$\frac{5\alpha_j^H}{1 + (\alpha_j^H)^2} \geq M^*(m, \ell, n) := 5\varphi(M_1(m, \ell, n)),$$

where

$$\varphi(\alpha) := \frac{\alpha}{1 + \alpha^2}, \quad M_1(m, \ell, n) := \frac{m + \sqrt{m^2 + 64}}{2(3 - 2p_n)}.$$

From these estimates, we have

$$\begin{aligned} D_i(\alpha_j^H) &> m[dp_i^2 - 3dp_i + M^*(m, \ell, n)] \\ &= m[dp_i(p_i - 3) + M^*(m, \ell, n)] \\ &\geq m \left[ -\frac{9}{4}d + M^*(m, \ell, n) \right]. \end{aligned}$$

Therefore, if we choose  $d$  so that

$$0 < d < \min \left\{ m^{-1}, \frac{4}{9}M^*(m, \ell, n) \right\} := d_*(m, \ell, n),$$

then  $D_i(\alpha_j^H) > 0$  for each  $i \in \mathbf{N}_0$ . Finally, let the eigenvalues close to the pure imaginary one near  $\alpha = \alpha_j^H$  be  $\gamma(\alpha) \pm i\omega(\alpha)$ . Then  $\gamma'(\alpha_j^H) = T'_j(\alpha_j^H)/2 = A'(\alpha_j^H)/2 > 0$ , since we have shown that  $A'(\alpha) > 0$  for all  $\alpha \geq \alpha_0$ . Hence, all the conditions in  $(H_1)$  are satisfied. Now we can apply the Hopf bifurcation theorem (see Lemma 5.1) to obtain the desired results.  $\square$

Next, we consider the bifurcation direction ( $\alpha'(0) > 0$  or  $< 0$ ) and stability of the bifurcating periodic solutions bifurcating from  $\alpha = \alpha_0^H$  according to [26].

**Theorem 2.2.** *Let  $\alpha_0^H$  be defined as in Theorem 2.1, and let the constant  $M_0 > 0$  be defined as*

$$M_0 = \frac{\sqrt{19\sqrt{769} - 147}}{2} \approx 9.7453.$$

Then, for system (2.1),

1. *If  $0 < m < M_0$ , then Hopf bifurcation at  $\alpha = \alpha_0^H$  is supercritical,  $\alpha(s) > \alpha_0^H$  for small  $s$ , and the bifurcating (spatially homogeneous) periodic solutions are locally asymptotically stable;*

2. *If  $m > M_0$ , then Hopf bifurcation at  $\alpha = \alpha_0^H$  is subcritical,  $\alpha(s) < \alpha_0^H$  for small  $s$ , and the bifurcating (spatially homogeneous) periodic solutions are unstable.*

*Proof.* Here we follow the notations and calculations in [26]. We set

$$\begin{cases} q := (a_0, b_0)^T = \left(1, \frac{3\alpha_0^2 - 5}{4\alpha_0} - i\frac{\omega_0(1 + \alpha_0^2)}{4\alpha_0}\right)^T, \\ q^* := (a_0^*, b_0^*)^T \\ = \left(\frac{1}{2\ell\pi} + i\frac{3\alpha_0^2 - 5}{2\omega_0\ell\pi(1 + \alpha_0^2)}, -i\frac{2\alpha_0}{\ell\pi\omega_0(1 + \alpha_0^2)}\right)^T, \end{cases}$$

where  $\omega_0 = \sqrt{(5m\alpha_0)/(1 + \alpha_0^2)}$ . By direct calculation, it follows that

$$\begin{cases} g_{uu} = \frac{m}{4}f_{uu}, \quad g_{uv} = \frac{m}{4}f_{uv}, \\ g_{uuu} = \frac{m}{4}f_{uuu}, \quad g_{uuv} = \frac{m}{4}f_{uuv}, \\ f_{vv} = f_{vvv} = f_{uvv} = g_{vv} = g_{uuv} = g_{vvv} = 0, \\ f_{uu} = \frac{8\alpha(3 - \alpha^2)}{(1 + \alpha^2)^2}, \quad f_{uv} = \frac{4(\alpha^2 - 1)}{(1 + \alpha^2)^2}, \\ f_{uuu} = \frac{24(\alpha^4 - 6\alpha^2 + 1)}{(1 + \alpha^2)^3}, \\ f_{uuv} = \frac{8\alpha(3 - \alpha^2)}{(1 + \alpha^2)^3}. \end{cases}$$

Then

$$\begin{cases} c_0 = -2\frac{\alpha_0^4 - 4\alpha_0^2 - 5}{\alpha_0(1 + \alpha_0^2)^2} - i\frac{2\omega_0(\alpha_0^2 - 1)}{\alpha_0(1 + \alpha_0^2)}, \\ d_0 = \frac{m}{4}c_0, \quad e_0 = -2\frac{\alpha_0^4 - 4\alpha_0^2 - 5}{\alpha_0(1 + \alpha_0^2)^2}, \\ f_0 = \frac{m}{4}e_0, \quad crg_0 = 6\frac{\alpha_0^4 - 10\alpha_0^2 - 11}{(1 + \alpha_0^2)^3} + i\frac{2\omega_0(\alpha_0^2 - 3)}{(1 + \alpha_0^2)^2}, \quad h_0 = \frac{m}{4}g_0, \end{cases}$$

and

$$\langle q^*, Q_{qq} \rangle = \langle \bar{q}^*, Q_{qq} \rangle = \frac{c_0}{2}, \langle q^*, Q_{q\bar{q}} \rangle = \langle \bar{q}^*, Q_{q\bar{q}} \rangle = \frac{e_0}{2}.$$

Hence,

$$\begin{aligned} H_{20} &= \begin{pmatrix} c_0 \\ d_0 \end{pmatrix} - \frac{c_0}{2} \begin{pmatrix} a_0 \\ b_0 \end{pmatrix} - \frac{c_0}{2} \begin{pmatrix} \bar{a}_0 \\ \bar{b}_0 \end{pmatrix} \\ &= c_0 \begin{pmatrix} 1 \\ m/4 \end{pmatrix} - c_0 \begin{pmatrix} 1 \\ (3\alpha_0^2 - 5)/(4\alpha_0) \end{pmatrix} = 0, \\ H_{11} &= \begin{pmatrix} e_0 \\ f_0 \end{pmatrix} - \frac{e_0}{2} \begin{pmatrix} a_0 \\ b_0 \end{pmatrix} - \frac{e_0}{2} \begin{pmatrix} \bar{a}_0 \\ \bar{b}_0 \end{pmatrix} \\ &= e_0 \begin{pmatrix} 1 \\ m/4 \end{pmatrix} - e_0 \begin{pmatrix} 1 \\ (3\alpha_0^2 - 5)/(4\alpha_0) \end{pmatrix} = 0, \end{aligned}$$

which implies that  $\omega_{20} = \omega_{11} = 0$ . Then

$$\langle q^*, Q_{\omega_{11}, q} \rangle = \langle q^*, Q_{\omega_{20}, \bar{q}} \rangle = 0.$$

Thus,

$$\begin{aligned} \text{Re}(c_1(\alpha_0^H)) &= \text{Re} \left\{ \frac{i}{2\omega_0} \langle q^*, Q_{qq} \rangle \cdot \langle q^*, Q_{q\bar{q}} \rangle + \frac{1}{2} \langle q^*, C_{q,q,\bar{q}} \rangle \right\} \\ (2.6) \quad &= -\frac{(\alpha_0^2 - 1)(\alpha_0^2 - 5)}{2\alpha_0^2(\alpha_0^2 + 1)^2} + \frac{3(\alpha_0^2 - 11)}{2(1 + \alpha_0^2)^2} \\ &= \frac{2\alpha_0^4 - 27\alpha_0^2 - 5}{2\alpha_0^2(1 + \alpha_0^2)^2}. \end{aligned}$$

From (2.6) and simple algebraic calculations, we know that if  $0 < m < M_0$ ,  $\text{Re}(c_1(\alpha_0^H)) < 0$ , and if  $m > M_0$ ,  $\text{Re}(c_1(\alpha_0^H)) > 0$ . From the proof of Theorem 2.1, we know that  $\gamma'(\alpha_0^H) > 0$ . Hence, we obtain the direction of bifurcation according to Lemma 5.1 in the Appendix.  $\square$

We make the following remarks for this section:

1. The bifurcation of spatially homogeneous periodic orbits at  $\alpha = \alpha_0^H$  has been considered in [24], where we used  $b$  (equivalent to  $m$  in (2.1)) in (1.1) as the bifurcation parameter.
2. In Theorem 2.2, if the Hopf bifurcation at  $\alpha = \alpha_0^H$  is supercritical, then the periodic orbit for  $\alpha > \alpha_0^H$  appears to be unique, see Figure 2.1

for phase portraits of  $m = 2$  and  $\alpha > \alpha_0^H$ . When  $\alpha$  is larger, the  $u$ -component of the limit cycle tends to have a zigzag profile, while the  $v$ -component appears to be hump shaped, see the solution curve in Figure 2.1. The pulse profile of the limit cycle in predator-prey model was recently studied by Hsu and Shi [5].

3. In Theorem 2.2, if the Hopf bifurcation at  $\alpha = \alpha_0^H$  is subcritical, then for  $\alpha \in (\alpha_0^H - \varepsilon, \alpha_0^H)$ , there exist two periodic orbits with the outer one being a limit cycle, see Figure 2.2 for phase portraits of  $m = 20$  and  $\alpha < \alpha_0^H$ . It appears that there exists an  $\alpha_*^H < \alpha_0^H$  such that the ODE system has two periodic orbits for  $\alpha \in (\alpha_*^H, \alpha_0^H)$ , there is a unique limit cycle for  $\alpha \geq \alpha_0^H$ , and all periodic orbits lie on a curve with a saddle-node bifurcation. The uniqueness or exact multiplicity of periodic orbits for either  $m < M_0$  or  $m \geq M_0$  is not known.

4. The bifurcation direction and the stability of the bifurcating periodic solutions for the spatially nonhomogeneous periodic orbits can also be determined by the formulae given in the Appendix or in [26]. However, the calculations are very lengthy; here, we leave them to the interested readers.

5. Since  $M_1(m, \ell, n) = (m + \sqrt{m^2 + 64})/4((3/2) - (n^2/\ell^2))^{-1}$ , then indeed  $M_1(m, \ell, n) = M_1(m, n^2/\ell^2)$ . Notice that an appropriate maximum  $n$  can be chosen by a fixed  $\ell$ , so  $M_1$  essentially depends only on  $m$  and  $\ell$ .

6. Theorem 2.1 is a great complement of [13, Theorem 1], in which it was shown that, for fixed  $\alpha$  and domain  $\Omega$ , if  $d$  is sufficiently small, then (2.1) has no nonconstant steady state solutions. Our results show that, when  $d$  is small, in spite of the nonexistence of steady state patterns, there possibly exist spatially homogenous and non-homogeneous oscillatory patterns. On the other hand, from the proof of Theorem 2.1, we show that  $D_i(\alpha_j^H) > 0$  for all  $i \in \mathbf{N}$ . Indeed, the proof works for any bounded  $\alpha$  if we make  $d$  small, which implies that, for any  $\alpha_M > 0$ , there is no steady state bifurcations for  $\alpha \in [0, \alpha_M]$  if we choose  $d$  small enough, and this agrees with the nonexistence result in [13, Theorem 1]. Combining the two results, one can say that, for any fixed  $\alpha > \alpha_0$ , if we choose  $d$  to be small enough, then there is only one (unstable spatially homogeneous) steady state but possibly many spatially nonhomogeneous periodic orbits.

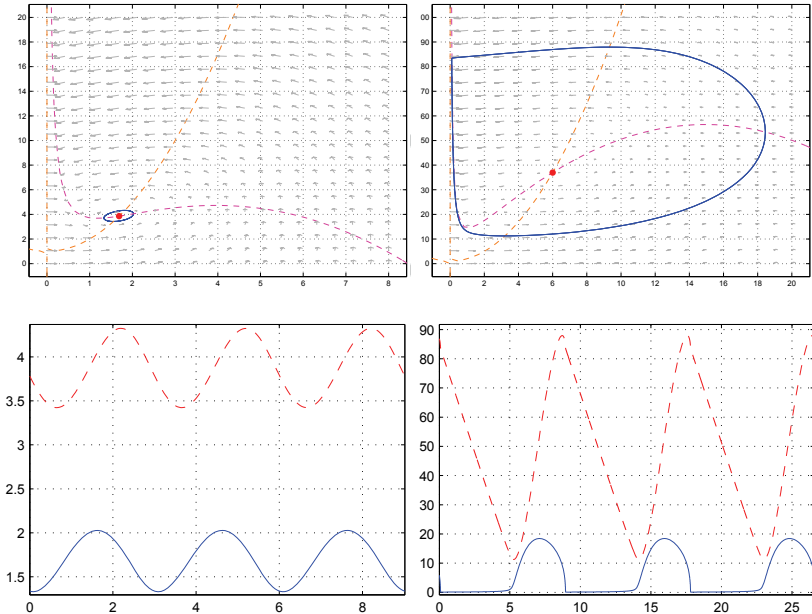


FIGURE 2.1. Phase portraits and solution curves for the ODE system corresponding to (2.1). Here,  $m = 2$ , the primary Hopf bifurcation point  $\alpha_0^H = 5/3 \approx 1.667$ , and it is supercritical. Left:  $\alpha = 1.69$ , one small amplitude limit cycle; Right:  $\alpha = 6$ , a large amplitude limit cycle; Top: phase portraits; Bottom: solution curves (solid curve  $u(t)$ , dotted curve:  $v(t)$ ).

**3. Steady state bifurcation analysis.** In this section we consider the steady state bifurcations of system (2.1). We consider the equations:

$$(3.1) \quad \begin{cases} u_{xx} + 5\alpha - u - \frac{4uv}{1+u^2} = 0 & x \in (0, \ell\pi), \\ dv_{xx} + u - \frac{uv}{1+u^2} = 0 & x \in (0, \ell\pi), \\ u_x(0) = v_x(0) = u_x(\ell\pi) = v_x(\ell\pi) = 0. \end{cases}$$

The existence of solutions to (3.1) has been considered in [13], and the related bifurcation problem has been discussed in [6]. Note that the bifurcations of steady state are independent of parameter  $m$ . It is known that, when  $\alpha$  is small, or  $d$  is small or  $\ell$  is small, then (3.1) has

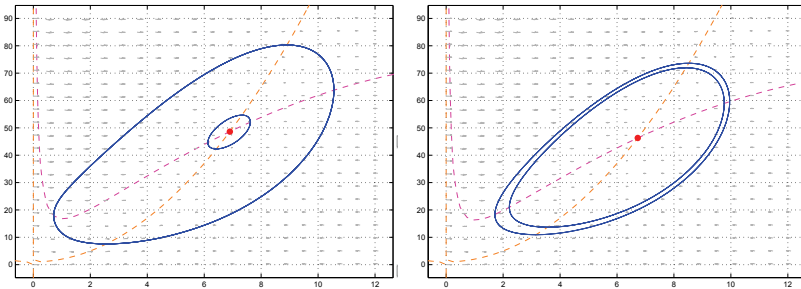


FIGURE 2.2. Phase portrait for the ODE system corresponding to (2.1). Here,  $m = 20$ , the primary Hopf bifurcation point  $\alpha_0^H \approx 6.908$ , and it is subcritical. Left:  $\alpha = 6.90$ , the small amplitude unstable periodic orbit is from Hopf bifurcation, and the larger one is stable; Right:  $\alpha = 6.73$ , two nearly identical periodic orbits when  $\alpha$  is close to the saddle-node bifurcation point ( $\approx 6.727$ ).

only the trivial constant solution  $(\alpha, \alpha^2 + 1)$ ; on the other hand, with some other appropriate conditions, (3.1) possesses a nontrivial solution if  $d$  is large (see [13]). In [6],  $d$  was used as bifurcation parameter, and it was shown that continua of nontrivial solutions of (3.1) exist in the space of  $(d, u, v)$ , which is unbounded in positive  $d$  direction but bounded in  $(u, v)$  due to the *a priori* estimates for fixed  $(\alpha, \ell)$ . In this section we continue the approach used in the previous section, and we use  $\alpha$  as the bifurcation parameter to consider the bifurcation of solutions of (3.1).

Now we identify steady state bifurcation value  $\alpha$ , which satisfies the steady state bifurcation condition

$(H_2)$ : there exists an  $n \in \mathbf{N}_0$  such that

$$D_n(\alpha) = 0, \quad T_n(\alpha) \neq 0, \quad \text{and} \quad T_j(\alpha) \neq 0, \quad D_j(\alpha) \neq 0 \text{ for } j \neq n;$$

and

$$\frac{d}{d\alpha} D_n(\alpha) \neq 0.$$

Clearly,  $D_0(\alpha) \neq 0$  for  $\alpha > 0$ ; hence, we only consider  $n \in \mathbf{N}$ . In the following we fix an arbitrary  $d > 0$ . To determine  $\alpha$ -values satisfying condition  $(H_2)$ , we notice that  $D_n(\alpha) = 0$  is equivalent to

$$(3.2) \quad D(\alpha, p) := d(1 + \alpha^2)p^2 - p[d(3\alpha^2 - 5) - \alpha] + 5\alpha = 0,$$

where  $p = n^2/\ell^2$ . Solving for  $\alpha$  from the equation and choosing the positive one, we obtain

$$(3.3) \quad \alpha_2(p) = \frac{p + 5 + \sqrt{(p + 5)^2 + 4d^2p^2(3 - p)(p + 5)}}{2dp(3 - p)}.$$

Define

$$(3.4) \quad \tilde{\ell}_n = n\sqrt{\frac{1}{3}}, \quad n = 0, 1, 2, \dots;$$

then, for any  $\ell > \tilde{\ell}_n$ , there exists a unique  $\alpha_n^S := \alpha_2(n^2/\ell^2)$  such that  $D_n(\alpha_n^S) = 0$ , where  $\alpha_2(\cdot)$  is defined in (3.3). These points  $\alpha_n^S$  are potential steady state bifurcation points.

To further study these possible bifurcation points, we also solve  $p$  from equation (3.2), and we have

$$(3.5) \quad p = p_{\pm}(\alpha) := \frac{d(3\alpha^2 - 5) - \alpha \pm \sqrt{[d(3\alpha^2 - 5) - \alpha]^2 - 20d\alpha(1 + \alpha^2)}}{2d(1 + \alpha^2)}.$$

We prove the following lemma:

**Lemma 3.1.** *The function  $\alpha_2 : (0, 3) \rightarrow \mathbf{R}^+$  defined in (3.3) has a unique critical point  $p_* \in (0, 3)$ , which is the global minimum of  $\alpha_2(p)$  on  $(0, 3)$ , and  $\lim_{p \rightarrow 0^+} \alpha_2(p) = \lim_{p \rightarrow 3^-} \alpha_2(p) = \infty$ . Consequently, for  $\alpha \geq \alpha_* := \alpha_2(p_*)$ ,  $p_{\pm}(\alpha)$  is well defined as in (3.5);  $p_+(\alpha)$  is monotone increasing and  $p_-(\alpha)$  is monotone decreasing; and  $p_+(\alpha_*) = p_-(\alpha_*)$ ,  $\sup_{\alpha > \alpha_*} p_+(\alpha) = \lim_{\alpha \rightarrow \infty} p_+(\alpha) = 3$ ,  $\inf_{\alpha > \alpha_*} p_-(\alpha) = \lim_{\alpha \rightarrow \infty} p_-(\alpha) = 0$ .*

*Proof.* Let  $D(\alpha, p)$  be defined as in (3.2). Then the set  $\Lambda := \{(\alpha, p) : \alpha > 0, p > 0\}$  is given by the curve  $\{(\alpha_2(p), p) : 0 < p < 3\}$ . We prove that  $\alpha_2(p)$  has a unique critical point. Differentiating  $D(\alpha_2(p), p) = 0$  twice and letting  $\alpha_2'(p) = 0$ , we obtain that

$$-2d\alpha_2^2(p) + 2dp(3 - p)\alpha_2(p)\alpha_2''(p) - (p + 5)\alpha_2''(p) - 2d = 0.$$

Thus,

$$\begin{aligned} \alpha_2''(p) &= \frac{2d(\alpha_2^2(p) + 1)}{2dp(3 - p)\alpha_2(p) - (p + 5)} \\ &= \frac{2d(\alpha_2^2(p) + 1)}{dp(p + 5)\alpha_2^{-1}(p) + dp(3 - p)\alpha_2(p)} > 0. \end{aligned}$$



Here in the last equality we use the equation

$$(3.6) \quad [dp(3 - p)\alpha_2(p) - (p + 5)]\alpha_2(p) = dp(p + 5),$$

which is from  $D(\alpha_2(p), p) \equiv 0$ . Therefore, for any critical point  $p$  of  $\alpha_2(p)$ , we must have  $\alpha_2''(p) > 0$ , and thus the critical point must be unique and a local minimum point.

It is easy to see that  $\lim_{p \rightarrow 0^+} \alpha_2(p) = \lim_{p \rightarrow 3^-} \alpha_2(p) = \infty$ ; hence, the unique critical point  $p_*$  is the global minimum point. Since (3.5) is also obtained by solving (3.2), then  $\Lambda = \{(\alpha_2(p), p) : 0 < p < 3\}$ , and the curves  $(\alpha, p_{\pm}(\alpha))$  are identical. Then the properties of  $\alpha_2(p)$  determine the monotonicity and limiting behavior of  $p_{\pm}$ .  $\square$

Now, from Lemma 3.1, it is possible that, for some  $i < j$ ,  $\alpha_2(p_i) = \alpha_2(p_j)$  and  $p_-(\alpha_i^S) = p_+(\alpha_j^S)$ . In this case, for  $\alpha = \alpha_i^S = \alpha_j^S$ , 0 is not a simple eigenvalue of  $L(\alpha)$ , and we shall not consider bifurcations at such points. We notice that, from the properties of  $p_{\pm}(\alpha)$  in Lemma 3.1, the multiplicity of 0 as an eigenvalue of  $L(\alpha)$  is at most 2. On the other hand, it is also possible that some  $\alpha_i^S = \alpha_j^H$ . So the dimension of center manifold of the equilibrium  $(u_{\alpha}, v_{\alpha})$  can be between 1 and 4.

We claim that there are only countably many  $\ell > 0$ ; in fact, only finitely many  $\ell \in (0, M)$  for any given  $M > 0$ , such that  $\alpha = \alpha_i^S = \alpha_j^S$  or  $\alpha_i^S = \alpha_j^H$  for these  $\ell$  and some  $i, j \in \mathbf{N}$ . Let  $E_n(\alpha, \ell) = \ell^4(1 + \alpha^2)D_n(\alpha)$  and  $F_n(\alpha, \ell) = \ell^2(1 + \alpha^2)T_n(\alpha)$ . Then, for any  $n \in \mathbf{N}$ ,  $E_n(\alpha, \ell)$  and  $F_n(\alpha, \ell)$  are polynomials of  $\alpha$  and  $\ell$  with real coefficients. Hence, on the  $(\alpha, \ell)$ -plane, the set  $q_n = \{(\alpha, \ell) : E_n(\alpha, \ell) = 0\}$  or  $p_n = \{(\alpha, \ell) : F_n(\alpha, \ell) = 0\}$  is the union of countable analytic curves. Moreover, we require  $\alpha \in [\alpha_*, \infty)$ ; then, for any  $M > 0$ , there are only finitely many  $i, j \in \mathbf{N}$  such that  $q_i \cap ([\alpha_*, \infty) \times [0, M]) \neq \emptyset$  and  $p_j \cap ([\alpha_*, \infty) \times [0, M]) \neq \emptyset$ . These finitely many  $q_i, p_j$  have only finitely many intersection points in  $[\alpha_*, \infty) \times [0, M]$  due to the analyticity, and thus the intersection points of different  $q_i, p_j$  in  $[\alpha_*, \infty) \times [0, \infty)$  is countable. We define

$$(3.7) \quad L^E = \{\ell > 0 : E_i(\alpha, \ell) = E_j(\alpha, \ell) \quad \text{or} \quad E_i(\alpha, \ell) = F_j(\alpha, \ell) \\ \text{for some } \alpha \in [\alpha_*, \infty), \text{ and } i, j \in \mathbf{N}\}.$$

Then the points  $L^E$  can be arranged as a sequence whose only limit point is  $\infty$ .

Hence, if  $\ell \in \mathbf{R} \setminus L^E$  and  $\alpha_j^S$  is well defined, then  $(H_2)$  is satisfied at  $\alpha = \alpha_j^S$ . Now we show that  $(d/d\alpha)D_j(\alpha_j^S) \neq 0$ . By direct calculation, we have

$$\begin{aligned} \frac{d}{d\alpha}D_j(\alpha_j^S) &= \frac{m}{1 + (\alpha_j^S)^2} \frac{\partial D}{\partial \alpha}(\alpha_j^S, p_j) \\ &= \frac{-m}{1 + (\alpha_j^S)^2} [2dp_j(3 - p_j)\alpha_j^S - (p_j + 5)] \\ &= \frac{-m}{1 + (\alpha_j^S)^2} [dp_j(p_j + 5)(\alpha_j^S)^{-1} + dp_j(3 - p_j)\alpha_j^S] < 0, \end{aligned}$$

by using (3.6), where  $p_j = j^2/\ell^2$ .

Summarizing the above discussions, and using a general bifurcation theorem (see Theorem 5.2 in the Appendix and [16]), we obtain the main result of this section on the global bifurcations of steady state solutions:

**Theorem 3.2.** *For any  $d > 0$ , if  $\ell \in (0, \infty) \setminus L^E$  and  $\tilde{\ell}_n < \ell < \tilde{\ell}_{n+1}$  for some  $n \in \mathbf{N}$ , where  $\tilde{\ell}_n$  is defined in (3.4) and  $L^E$  is a countable subset of  $\mathbf{R}^+$  defined in (3.7), then there exist  $n$  points  $\alpha_j^S = \alpha_j^S(d, \ell)$ ,  $1 \leq j \leq n$ , satisfying*

$$\alpha_* < \alpha_1^S < \alpha_2^S < \dots < \alpha_n^S < \infty,$$

with  $\alpha_j^S = \alpha_2(j^2/\ell^2)$  or, equivalently,  $p_{\pm}(\alpha_j^S) = j^2/\ell^2$ , and  $\alpha = \alpha_n^S$  is a bifurcation point for (3.1). Moreover,

1. *There exists a  $C^\infty$  smooth curve  $\Gamma_j$  of solutions of (3.1) bifurcating from  $(\alpha, u, v) = (\alpha_j^S, u_{\alpha_j^S}, v_{\alpha_j^S})$ , with  $\Gamma_j$  contained in a global branch  $\mathcal{C}_j$  of solutions of (3.1);*

2. *Near  $(\alpha, u, v) = (\alpha_j^S, u_{\alpha_j^S}, v_{\alpha_j^S})$ ,  $\Gamma_j = \{(\alpha_j(s), u_j(s), v_j(s)) : s \in (-\varepsilon, \varepsilon)\}$ , where  $u_j(s) = \alpha_j^S + \mathbf{s}\mathbf{a}_j \cos(jx/\ell) + s\psi_{1,j}(s)$ ,  $v_j(s) = (1 + \alpha_j^S)^2 + \mathbf{s}\mathbf{b}_j \cos(jx/\ell) + s\psi_{2,j}(s)$  for  $s \in (-\varepsilon, \varepsilon)$  for some  $C^\infty$  smooth functions  $\alpha_j, \psi_{1,j}, \psi_{2,j}$  such that  $\alpha_j(0) = \alpha_j^S$  and  $\psi_{1,j}(0) = \psi_{2,j}(0) = 0$ . Here  $\mathbf{a}_j$  and  $\mathbf{b}_j$  satisfy*

$$L(\alpha_j^S)[(\mathbf{a}_j, \mathbf{b}_j)^T \cos(nx/\ell)] = (0, 0)^T.$$

3. Each  $\mathcal{C}_j$  is unbounded, that is, the projection of  $\mathcal{C}_j$  on the  $\alpha$ -axis contains  $(\alpha_j^S, \infty)$ .

*Proof.* To apply Theorem 5.2, one only needs to show the local conditions  $(H_2)$  and  $(d/d\alpha)D_j(\alpha_j^S) \neq 0$ , which have been proved in previous paragraphs. Note that we exclude  $L^E$  so  $\alpha = \alpha_j^S$  is always a bifurcation from a simple eigenvalue point. Thus, the results stated here except the unboundedness of  $\mathcal{C}_j$  follow from Theorem 5.2 in the Appendix or [16].

We follow an argument in [6], as well as an earlier work of Nishiura [14] and Takagi [18], to prove that  $\mathcal{C}_j$  is unbounded. From the results of [13, 25], (3.1) has no non-constant solutions, and [13, Proposition 2.2] shows that all non-constant solutions of (3.1) satisfy  $0 < u(x) < 5\alpha$  and  $0 < v(x) < 1 + 25\alpha^2$ . That implies that  $\mathcal{C}_j$  must remain bounded for finite  $\alpha$ . Suppose that the projection of  $\mathcal{C}_j$  in  $\alpha$ -axis is bounded. Then  $\mathcal{C}_j$  must contain another bifurcation point  $(\alpha_i^S, \alpha_i^S, 1 + (\alpha_i^S)^2)$  for some  $i \neq j$  from Theorem 5.2. Indeed,  $\mathcal{C}_j$  contains finitely many bifurcation points in form of  $(\alpha_i^S, \alpha_i^S, 1 + (\alpha_i^S)^2)$ , since there are only finitely  $i \in \mathbf{N}$  such that  $i^2/\ell^2 < 3$  for fixed  $\ell > 0$ . Among these finitely many  $\alpha_i^S$ , there is one with the largest index  $i_M$ . Notice that equation (3.1) is also well defined for the interval  $(0, \ell\pi/i_M)$ , and the bifurcation points (depending on the length) have the relation

$$\alpha_{i_M}^S(\ell\pi) = \alpha_2(i_M^2/\ell^2) = \alpha_1^S(\ell\pi/i_M) := \alpha^M.$$

Hence,  $\alpha^M$  is also a bifurcation point for equation (3.1) with interval  $(0, \ell\pi/i_M)$ . From the global bifurcation theorem, the global branch  $\mathcal{C}_1^M$  bifurcating from  $\alpha = \alpha^M$  for equation (3.1) with interval  $(0, \ell\pi/i_M)$  is also unbounded or contains another bifurcation point. But any solution of (3.1) with interval  $(0, \ell\pi/i_M)$  can be extended to  $(0, \ell\pi)$  by reflection; hence, that  $\mathcal{C}_1^M$  is unbounded implies that  $\mathcal{C}_j$  is unbounded, which contradicts our assumption. Or  $\mathcal{C}_1^M$  contains another bifurcation point  $\alpha_k^S(\ell\pi/i_M)$ , but that will imply  $\alpha_{ki_M}^S(\ell\pi) = \alpha_k^S(\ell\pi/i_M)$  is on the branch  $\mathcal{C}_j$ , and clearly  $ki_M > i_M$  since  $k > 1$ , which contradicts with the maximality of  $i_M$ . Therefore, the projection of  $\mathcal{C}_j$  in  $\alpha$ -axis is not bounded.  $\square$

The unboundedness of the solution component  $\mathcal{C}_j$  implies the existence of at least one non-constant solution for  $\alpha > \min\{\alpha_i^S\}$  except at  $\alpha_i^S$  if  $\ell \notin L^E$ . Since the set of bifurcation points is finite here, we can state the following result regarding the existence of steady state solutions:

**Corollary 3.3.** *For any  $d > 0$  and  $\ell > 0$  except  $\ell \in L^E$ , there exists an  $\alpha_M := \alpha_M(d, \ell) > 0$  such that, when  $\alpha > \alpha_M$ , (3.1) possesses at least one non-constant steady state solution.*

Note that  $\ell \notin L^E$  is only technical and, for  $\ell \in L^E$ , as long as there is one bifurcation point that is simple, then the existence still holds. We also remark that, at each bifurcation point,  $\alpha = \alpha_j^S$ , the steady state bifurcation is a pitchfork one so that  $\alpha_j'(0) = 0$ . This is natural since  $(u(\ell\pi - x), v(\ell\pi - x))$  is also a solution if  $(u(x), v(x))$  is a solution. The direction of the bifurcation thus is determined by  $\alpha_j''(0)$ . In Lemma 5.3 in the Appendix, we show that  $\alpha_j''(0)$  can be calculated, so one can determine whether it is a supercritical or subcritical pitchfork bifurcation.

We conclude this section by discussing the relation between Hopf bifurcations and steady state bifurcations. We can look at a fixed eigenmode  $\cos(nx/\ell)$ , and the bifurcations related to this mode have the following possible scenarios:

(Case 1) If  $\ell \leq n/\sqrt{3}$ , then neither  $\alpha_n^H$  nor  $\alpha_n^S$  exists, and there is no bifurcation for this mode;

(Case 2) If  $n/\sqrt{3} < \ell \leq n\sqrt{(1+md)/3}$ ,  $\alpha_n^S$  exists but not  $\alpha_n^H$ , then there exists only a steady state bifurcation but no Hopf bifurcation for this eigenmode;

(Case 3) If  $\ell > n\sqrt{(1+md)/3}$ , then both of  $\alpha_n^S$  and  $\alpha_n^H$  exist. Now there are two subcases:

(a) If  $\alpha_n^H < \alpha_n^S$ , then there are one steady state bifurcation at  $\alpha = \alpha_n^S$  and one Hopf bifurcation at  $\alpha = \alpha_n^H$ ;

(b) If  $\alpha_n^S < \alpha_n^H$ , then there is a steady state bifurcation at  $\alpha = \alpha_n^S$  but no Hopf bifurcation as  $D_n(\alpha) < 0$  at  $\alpha_n^H$ .

In fact, Case 3 (a) above suggests a more general Hopf bifurcation theorem than the one in Theorem 2.1:

**Theorem 3.4.** *Suppose that  $n \in \mathbf{N}$ ,  $m, d > 0$ , and*

$$(3.8) \quad \ell > \sqrt{\frac{1+md}{3}}n.$$

*If*

$$(3.9) \quad \begin{aligned} \alpha_n^H &:= \frac{m + \sqrt{m^2 + 4(3 - \tilde{p})(5 + \tilde{p})}}{2(3 - \tilde{p})} \\ &< \frac{p + 5 + \sqrt{(p + 5)^2 + 4d^2p^2(3 - p)(p + 5)}}{2dp(3 - p)} \\ &:= \alpha_n^S, \end{aligned}$$

where  $\tilde{p} = (1 + md)n^2/\ell^2$  and  $p = n^2/\ell^2$ , and  $\alpha_n^H \neq \alpha_j^S$  for  $j \neq n$ , then system (2.1) undergoes a Hopf bifurcation at  $\alpha = \alpha_n^H$ , and the bifurcating periodic solutions satisfy the description in Theorem 2.1. In particular, this occurs for any given  $d > 0$  and  $\ell > n/\sqrt{3}$ , and  $m > 0$  is chosen to be small so that (3.9) is satisfied.

*Proof.* If the conditions stated are satisfied, then  $(H_1)$  and (2.3) are satisfied; thus, Hopf bifurcation occurs as in Theorem 2.1. If we choose  $m$  small enough, then (3.8) is satisfied if  $\ell > n/\sqrt{3}$ , and  $\alpha_n^H(m) < \alpha_n^S$  since  $\tilde{p} \rightarrow p$  and  $\alpha_n^H(m) \rightarrow \sqrt{(3 - p)(p + 5)}/(3 - p) < \alpha_n^S$ .  $\square$

**4. Examples and numerical simulations.** We use some examples of parameters to illustrate different bifurcation diagrams. In the following, we use the graphs of

$$T(\alpha, p) := \frac{3\alpha^2 - m\alpha - 5}{1 + \alpha^2} - p(1 + md) = 0, \quad (\text{Hopf})$$

and

$$\begin{aligned} D(\alpha, p) &:= d(1 + \alpha^2)p^2 - p[d(3\alpha^2 - 5) - \alpha] \\ &+ 5\alpha = 0, \quad (\text{steady state}) \end{aligned}$$

as bifurcation diagrams, see Figures 4.1 and 4.3. In these bifurcation diagrams, the horizontal lines are  $p = p_n := n^2/\ell^2$ ; the monotone

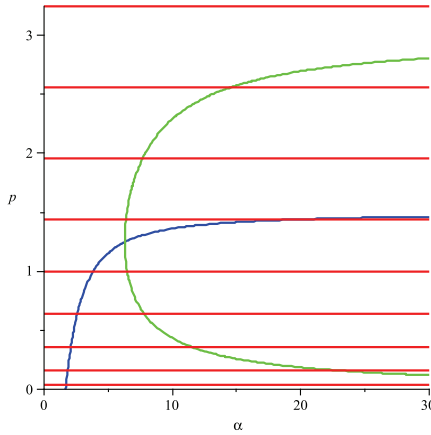


FIGURE 4.1. Graph of  $T(\alpha, p) = 0$  and  $D(\alpha, p) = 0$ . Here  $m = 2$ ,  $d = 0.5$  and  $\ell = 5$ . The horizontal lines are  $p = n^2/\ell^2$  where  $1 \leq n \leq 9$ . In this case  $\alpha_* > \alpha_0^H$ , and Hopf bifurcations occur before steady state bifurcations.

increasing curve is  $T(\alpha, p) = 0$ , and the parabola-like curve is  $D(\alpha, p) = 0$ . The  $\alpha$ -value of each intersection of  $T(\alpha, p) = 0$  with a horizontal line  $p = p_n$  is a potential Hopf bifurcation point; and the intersection of  $D(\alpha, p) = 0$  with  $p = p_n$  is a possible steady state bifurcation. The primary Hopf bifurcation point is  $\alpha_0 = (m + \sqrt{m^2 + 60})/6$ .

**Example 4.1.** In Figure 4.1, we set  $m = 2$ ,  $d = 0.5$  and  $\ell = 5$ . The primary Hopf bifurcation point is  $\alpha_0^H = 5/3 = 1.667$ , and the minimum  $\alpha_* \approx 6.283$  on  $D(\alpha, p) = 0$  is larger than  $\alpha_0^H$ .

All four cases of order of bifurcations listed at the end of Section 3 could happen for this set of parameters. For  $1 \leq n \leq 5$ , Case 3 (a) occurs: there exists a true Hopf bifurcation point and a true steady state bifurcation point. For  $n = 6$ , Case 3 (b) occurs: there exists a true steady state bifurcation point, but the Hopf bifurcation point does not occur. For  $n = 7$  and  $n = 8$ , Case 2 occurs: there exists only a steady state bifurcation point but no Hopf bifurcation points. For  $n > 8$ , Case 1 occurs: no bifurcation. More precisely,

$$\begin{aligned} \alpha_0^H \approx 1.667 < \alpha_1^H \approx 1.705 < \alpha_2^H \approx 1.831 \\ < \alpha_3^H \approx 1.2082 < \alpha_4^H \approx 2.579 < \alpha_5^H \approx 3.828 < \alpha_6^H \approx 19.96, \end{aligned}$$

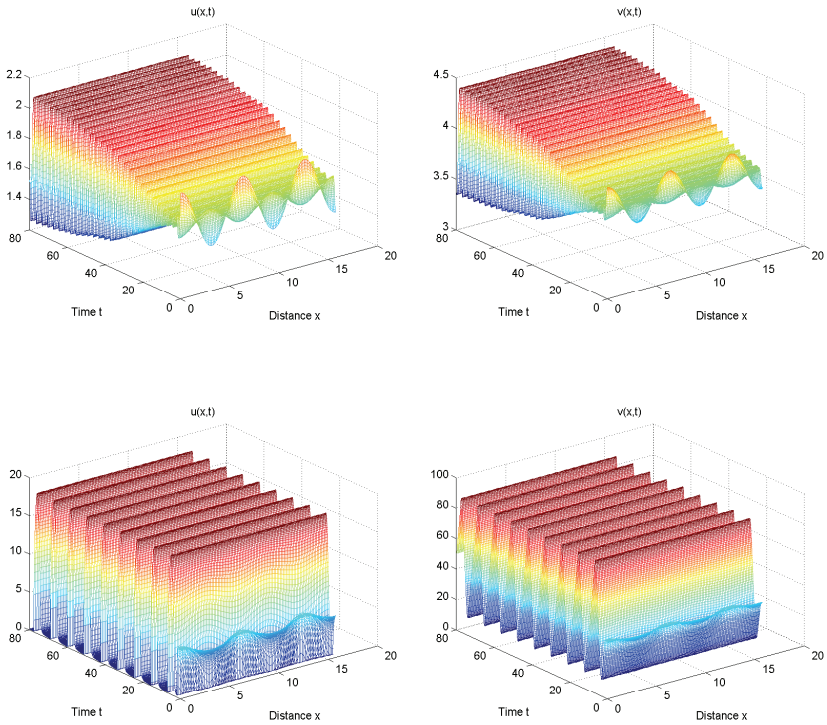


FIGURE 4.2. Numerical simulation of the system (2.1). Here  $m = 2$ ,  $d = 0.5$ ,  $\ell = 5$ . Left: Graph of  $u(x, t)$ . Right: Graph of  $v(x, t)$ ; Top:  $\alpha = 1.69 > \alpha_0^H \approx 1.667$  and the initial values  $u_0(x) = 1.7 + 0.2 \cos x$  and  $v_0(x) = (1.7^2 + 1) + 0.2 \cos x$ . The solution tends to the spatially homogenous periodic orbit; Bottom:  $\alpha = 6 < \alpha_* \approx 6.283$  and the initial values  $u_0(x) = 6 + 0.5 \cos x$  and  $v_0(x) = (6^2 + 1) + 0.5 \cos x$ . The solution tends to the large amplitude spatially homogenous periodic orbit.

( $\alpha_6^H$  is not a true Hopf bifurcation point), and

$$\begin{aligned}
 \alpha_1^S &\approx 85.16 > \alpha_2^S \approx 22.79 > \alpha_8^S \approx 14.6 > \alpha_3^S \\
 &\approx 11.46 > \alpha_4^S \approx 7.776 > \alpha_7^S \approx 7.693 \\
 &> \alpha_5^S \approx 6.464 > \alpha_6^S \approx 6.382.
 \end{aligned}$$

For this parameter set, there are six Hopf bifurcation points all less than  $\alpha_* \approx 6.283$ , and there are eight steady state bifurcation points all

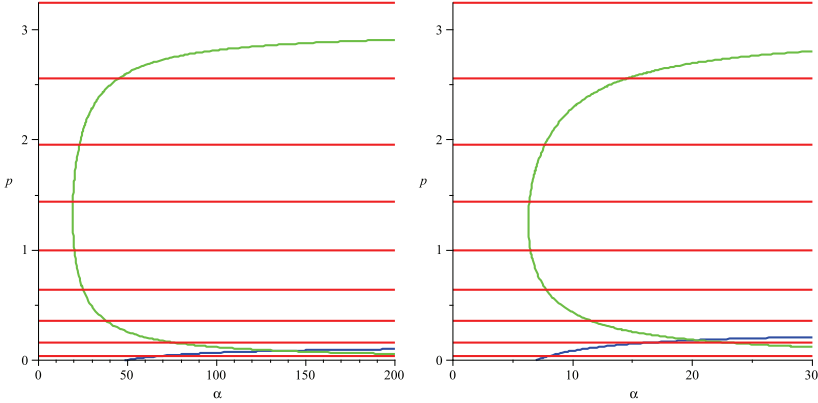


FIGURE 4.3. Graph of  $T(\alpha, p)$  and  $D(\alpha, p) = 0$ . (A) Left:  $m = 145$ ,  $d = 0.15$  and  $\ell = 5$ ; (B) Right:  $m = 20$ ,  $d = 0.5$  and  $\ell = 5$ .

larger than  $\alpha_*$ . From Theorem 2.2, the Hopf bifurcation at  $\alpha = \alpha_0^H$  is supercritical, and the bifurcating (spatially homogeneous) periodic solutions are locally asymptotically stable since  $0 < m < M_0$ .

Two numerical simulations are shown in Figure 4.2 for the cases of  $\alpha = 1.69$  and  $\alpha = 6$  and, in both cases, the solutions converge to the spatially homogenous periodic orbit (see Figure 2.1 for the corresponding phase portraits and solution curves). In both cases, the initial value is a non-constant perturbation of the constant steady state.

**Example 4.2.** In Figure 4.3 (A), we set  $m = 145$ ,  $d = 0.15$ ,  $\ell = 5$ . We have:

$$\begin{aligned} \alpha_0^H &\approx 48.37 < \alpha_1^H \approx 69.42, \\ \alpha_1^S &\approx 283.8 > \alpha_2^S \approx 75.73 > \alpha_8^S \approx 45.11 > \alpha_3^S \approx 37.64 > \alpha_4^S \approx 24.99 \\ &> \alpha_7^S \approx 23.06 > \alpha_5^S \approx 20.15 > \alpha_6^S \approx 19.32, \end{aligned}$$

and

$$\alpha_* \approx 19.20 < \alpha_0^H \approx 48.37.$$



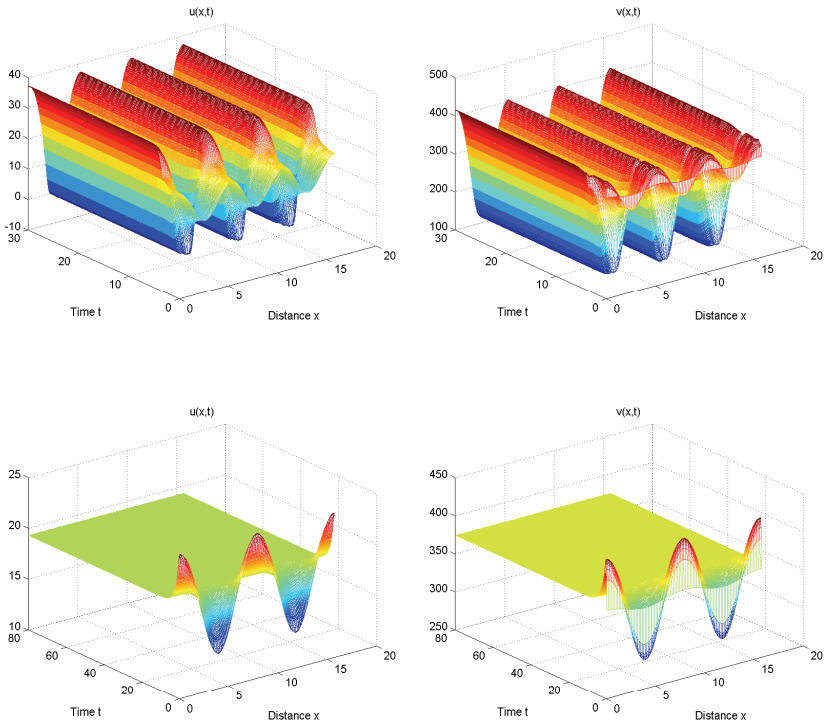


FIGURE 4.4. Numerical simulation of system (2.1). Here  $m = 145$ ,  $d = 0.15$ ,  $\ell = 5$  and  $19.32 \approx \alpha_6^S < \alpha = 19.33 < \alpha_0^H \approx 48.37$ . Left: Graph of  $u(x, t)$ . Right: Graph of  $v(x, t)$ ; Top: the initial values  $u_0(x) = 19 + 5 \cos(6x/5)$ ,  $v_0(x) = (19^2 + 1) + 5 \cos(6x/5)$ , and the solution tends to a spatially nonhomogeneous steady state with mode  $\cos(6x/5)$ ; Bottom: the initial values  $u_0(x) = 19 + 5 \cos(4x/5)$ ,  $v_0(x) = (19^2 + 1) + 5 \cos(4x/5)$ , and the solution tends to the constant steady state.

In this example  $\alpha_* < \alpha_0$ , and some Turing bifurcations occur for  $\alpha < \alpha_0$ . When  $\alpha$  increases, the first bifurcation point is  $\alpha_6^S \approx 19.32$ . Some numerical simulations are shown for  $\alpha = 19.33$ , see Figure 4.4.

In this case, it appears that two stable steady states exist: the constant one  $(\alpha, 1 + \alpha^2)$ , and one with eigenmode  $\cos(6x/5)$ . Figure 4.4 demonstrates the convergence to either steady state. Indeed, one can notice that the steady state with eigenmode  $\cos(6x/5)$  is a large amplitude one. This is caused by a subcritical pitchfork bifurcation

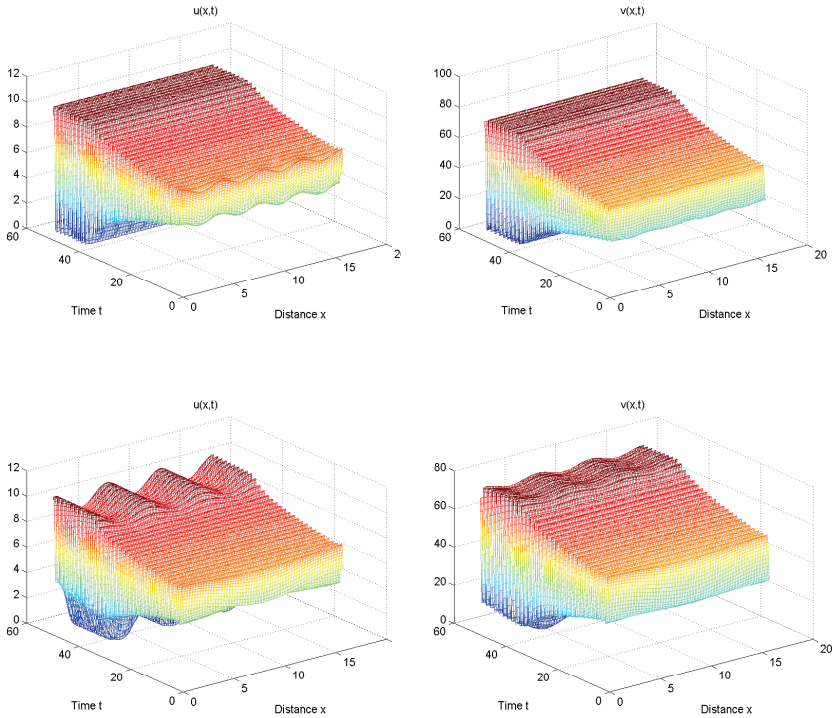


FIGURE 4.5. Numerical simulation of system (2.1). Here  $m = 20$ ,  $d = 0.5$ ,  $\ell = 5$  and  $6.382 \approx \alpha_6^S < \alpha = 6.9 < \alpha_0^H \approx 6.908$ . Left: Graph of  $u(x, t)$ . Right: Graph of  $v(x, t)$ ; Top: the initial values  $u_0(x) = 6 + 0.5 \cos(8x/5)$ ,  $v_0(x) = (6^2 + 1) + 0.5 \cos(8x/5)$ , and the solution tends to a spatially homogeneous time periodic orbit; Bottom: the initial values  $u_0(x) = 6 + 0.5 \cos(2x/5)$ ,  $v_0(x) = (6^2 + 1) + 0.5 \cos(2x/5)$ , and the solution tends to the spatially nonhomogeneous time periodic orbit.

occurring at  $\alpha = \alpha_6^S$ . By using the algorithm in the Appendix, one can show that  $\alpha_6''(0) = -0.3386$ , and further numerical simulations suggest that a stable steady state with eigenmode  $\cos(6x/5)$  exists for  $\alpha > 17.47$ . For  $\alpha < 17.47$ , the constant steady state appears to be the global attractor.

**Example 4.3.** In Figure 4.3 (B), we set  $m = 20$ ,  $d = 0.5$  and  $\ell = 5$ . The bifurcation points in this case are

$$\alpha_0^H \approx 6.908 < \alpha_1^H \approx 8.076, \alpha_2^S \approx 22.79 > \alpha_8^S \approx 14.6 > \alpha_3^S \approx 11.46 \\ > \alpha_4^S \approx 7.776 > \alpha_7^S \approx 7.693 > \alpha_5^S \approx 6.464 > \alpha_6^S \approx 6.382,$$

and

$$\alpha_* \approx 6.283.$$

Here we notice that  $m > M_0$ ; thus, the primary Hopf bifurcation is subcritical, and there exist two spatially homogenous periodic orbits for  $6.73 \leq \alpha < 6.908 = \alpha_0^H$  (see Figure 2.2). At  $\alpha = 6.9$ , the large amplitude spatially homogeneous periodic orbit appear as a stable pattern (see the top one in Figure 4.5), but a surprising pattern is a spatially nonhomogeneous periodic orbit with eigenmode  $\cos(6x/5)$  (see the bottom one in Figure 4.5). The nonhomogeneous periodic orbit with mode  $\cos(6x/5)$  cannot bifurcate from the constant steady state as only  $\alpha_0^H$  and  $\alpha_1^H$  exist here. However,  $\alpha_6^S \approx 6.382$  is a steady state bifurcation point, and we suspect that Hopf bifurcation could occur on the branch of steady state solutions with mode  $\cos(6x/5)$ . This is not covered by the theory we present here.

From these examples, we make some general remarks on the bifurcation diagrams of (2.1).

1. The parameter  $\ell$  determines the number of possible eigenmodes regardless of  $d$  and  $m$ . For larger  $\ell$ , bifurcations with more spatial modes are possible.

2. For a fixed  $\ell$ , the number  $n$  of possible eigenmodes is fixed. Then a steady state bifurcation with each of these eigenmodes occurs at  $\alpha = \alpha_j^S$  (unless they overlap), but Hopf bifurcation points could be fewer if  $md$  is large. On the other hand, on bifurcation diagrams like Figures 4.1 and 4.3, not every intersection of the Hopf bifurcation curve  $T(\alpha, p) = 0$  and horizontal line  $p = p_j$  produces a true Hopf bifurcation point. Now Theorem 3.4 can be interpreted as: if an intersection of the Hopf bifurcation curve  $T(\alpha, p) = 0$  and horizontal line  $p = p_j$  is outside of the curve  $D(\alpha, p) = 0$ , then it is a true Hopf bifurcation point, otherwise it is not.

3. The combined influence of parameters  $m$  and  $d$  changes the nature of the bifurcation diagram. For fixed  $m$ , decreasing  $d$  will “push”

the curve  $D(\alpha, p) = 0$  to the right, so most or all potential Hopf bifurcation points are outside of the curve  $D(\alpha, p) = 0$ . This is just another interpretation of Theorem 2.1. For the case of small  $d$ , the Hopf bifurcations occur at smaller  $\alpha$  (but larger than  $\alpha_0$ ), and all steady state bifurcations occur at large  $\alpha$ . But, for large  $d$ , intervening Hopf and steady state bifurcations could generate more complicated spatiotemporal patterns as shown in Examples 4.2 and 4.3.

**5. Concluding remarks.** The Hopf and steady state bifurcation analysis here makes another step toward a complete understanding of the global dynamics of the Lengel-Epstein model of CIMA reaction. We use a new bifurcation parameter  $\alpha$ , the rescaled feed concentration of  $I^-$ , in this article, which turns out to be the most important barometer of the system. We summarize the previous and new results regarding (2.1) with parameter  $\alpha$  and fixed  $d, m > 0$ : (recall that  $(u_\alpha, v_\alpha) = (\alpha, \alpha^2 + 1)$  is the unique positive constant steady state)

1. For  $0 < \alpha < \sqrt{27}/5 \approx 1.0392$ ,  $(u_\alpha, v_\alpha)$  is globally asymptotically stable ([25] and Theorem 2.3);

2. For  $\sqrt{27}/5 < \alpha < \sqrt{5/3} \approx 1.2910$ ,  $(u_\alpha, v_\alpha)$  is locally asymptotically stable, and there is no other known patterned solution;

3. For  $\sqrt{5/3} < \alpha < \alpha_0 := (\sqrt{m^2 + 60} + m)/6$ ,  $(u_\alpha, v_\alpha)$  is locally asymptotically stable for the ODE dynamics but could be unstable for PDE dynamics if  $d$  is small ([15, Lemma 5.1]); Turing bifurcation from  $(u_\alpha, v_\alpha)$  occurs if  $d$  decreases ([7, Theorem 3.4]) or  $\alpha$  increases (Theorem 3.2); no Hopf bifurcation is possible for  $\alpha$  in this range;

4.  $\alpha = \alpha_0$  is the smallest Hopf bifurcation point, where a spatially homogenous periodic orbit bifurcates from  $(u_\alpha, v_\alpha)$ , and for any  $\alpha > \alpha_0$ , a spatially homogenous periodic orbit exists (Theorem 2.1);

5. For  $\alpha > \alpha_0$ ,  $(u_\alpha, v_\alpha)$  is unstable even for the ODE dynamics; if  $\ell$  is small, no spatial (steady state or periodic) patterns exist, and each solution converges to a spatially homogenous periodic orbit ([25, Theorem 2.6]); if  $\ell$  is not small, then finitely many steady state and Hopf bifurcations are possible depending on the length  $\ell\pi$  of the interval (Theorems 2.1, 3.2, 3.4). If  $d$  is small, then  $(u_\alpha, v_\alpha)$  is the unique steady state for  $\alpha \in [\alpha_0, \alpha_M]$  for some  $\alpha_M > 0$  ([15, Theorem 1]), but the system could have a large number of periodic orbits for  $\alpha$  in that range (Theorems 2.1, 3.4); for  $\alpha > \alpha_M$ , the system possesses at least one nonhomogeneous steady state (Theorem 3.2 and Corollary 3.3).

APPENDIX

In this Appendix, we recall some known bifurcation results on the general reaction-diffusion equations in one dimensional space (see [26] for details). Consider

$$(5.1) \quad \begin{cases} u_t - d_1 u_{xx} = f(\alpha, u, v), & v_t - d_2 v_{xx} = g(\alpha, u, v), \\ x \in (0, \ell\pi), & t > 0, \\ u_x(0, t) = u_x(\ell\pi, t) = v_x(0, t) = v_x(\ell\pi, t) = 0 \end{cases}$$

where  $d_1, d_2, \alpha \in \mathbf{R}^+$ ,  $f, g : \mathbf{R} \times \mathbf{R}^2 \rightarrow \mathbf{R}$  are  $C^{k+2}$  ( $k \geq 2$ ), with  $f(\alpha, 0, 0) = g(\alpha, 0, 0) = 0$ . The corresponding steady state equation of (5.1) is

$$(5.2) \quad \begin{cases} -d_1 u_{xx} = f(\alpha, u, v), & -d_2 v_{xx} = g(\alpha, u, v) & x \in (0, \ell\pi), \\ u_x(0) = u_x(\ell\pi) = v_x(0) = v_x(\ell\pi) = 0. \end{cases}$$

Define the real-valued Sobolev space

$$X := \{(u, v) \in H^2(0, \ell\pi) \times H^2(0, \ell\pi) \mid (u_x, v_x)|_{x=0, \ell\pi} = 0\}.$$

and define the complexification of  $X$  to be  $X_{\mathbf{C}} := X \oplus iX = \{x_1 + ix_2 \mid x_1, x_2 \in X\}$  if necessary. We also define  $Y = L^2(0, \ell\pi) \times L^2(0, \ell\pi)$ . The linearized operator of system (5.2) evaluated at  $(\alpha, 0, 0)$ , is

$$L(\alpha) := \begin{pmatrix} d_1 \partial^2 / \partial x^2 + A(\alpha) & B(\alpha) \\ C(\alpha) & d_2 \partial^2 / \partial x^2 + D(\alpha) \end{pmatrix},$$

with the domain  $D_{L(\alpha)} = X$  (or  $X_{\mathbf{C}}$ ), where  $A(\alpha) = f_u(\alpha, 0, 0)$ ,  $B(\alpha) = f_v(\alpha, 0, 0)$ ,  $C(\alpha) = g_u(\alpha, 0, 0)$ , and  $D(\alpha) = g_v(\alpha, 0, 0)$ . Accordingly, we define,

$$L_n(\alpha) := \begin{pmatrix} -d_1 n^2 / \ell^2 + A(\alpha) & B(\alpha) \\ C(\alpha) & -d_2 n^2 / \ell^2 + D(\alpha) \end{pmatrix}.$$

To consider the Hopf bifurcation, we assume that, for some  $\alpha_0 \in \mathbf{R}$ , the following condition holds:

( $H_3$ ) There exists a neighborhood  $O$  of  $\alpha_0$  such that, for  $\alpha \in O$ ,  $L(\alpha)$  has a pair of complex, simple, conjugate eigenvalues  $\gamma(\alpha) \pm i\omega(\alpha)$ ,

continuously differentiable in  $\alpha$ , with  $\gamma(\alpha_0) = 0, \omega(\alpha_0) = \omega_0 > 0$ , and  $\gamma'(\alpha_0) \neq 0$ ; all other eigenvalues of  $L(\alpha)$  have non-zero real parts for  $\alpha \in O$ .

We assume that  $(H_3)$  holds. Then, by  $(H_3)$ , we can assume  $q = (a_n, b_n)^T \cos(n/\ell)x$ , with  $a_n, b_n \in \mathbf{C}$ , such that  $L(\alpha_0)q = i\omega_0 q$ . Define  $Q_{qq}, Q_{q\bar{q}}$  and  $C_{q,q,\bar{q}}$ :

$$\begin{aligned} Q_{q,q} &= \begin{pmatrix} c_n \\ d_n \end{pmatrix} \cos^2 \frac{n}{\ell}x, \\ Q_{q,\bar{q}} &= \begin{pmatrix} e_n \\ f_n \end{pmatrix} \cos^2 \frac{n}{\ell}x, \\ C_{q,q,\bar{q}} &= \begin{pmatrix} g_n \\ h_n \end{pmatrix} \cos^3 \frac{n}{\ell}x, \end{aligned}$$

where

$$\begin{cases} c_n = f_{uu}a_n^2 + 2f_{uv}a_nb_n + f_{vv}b_n^2, \\ d_n = g_{uu}a_n^2 + 2g_{uv}a_nb_n + g_{vv}b_n^2, \\ e_n = f_{uu}|a_n|^2 + f_{uv}(a_n\bar{b}_n + \bar{a}_nb_n) + f_{vv}|b_n|^2, \\ f_n = g_{uu}|a_n|^2 + g_{uv}(a_n\bar{b}_n + \bar{a}_nb_n) + g_{vv}|b_n|^2, \\ g_n = f_{uuu}|a_n|^2a_n + f_{uuv}(2|a_n|^2b_n + a_n^2\bar{b}_n) \\ \quad + f_{uvv}(2|b_n|^2a_n + b_n^2\bar{a}_n) + f_{vvv}|b_n|^2b_n, \\ h_n = g_{uuu}|a_n|^2a_n + g_{uuv}(2|a_n|^2b_n + a_n^2\bar{b}_n) \\ \quad + g_{uvv}(2|b_n|^2a_n + b_n^2\bar{a}_n) + g_{vvv}|b_n|^2b_n, \end{cases}$$

with all the partial derivatives of  $f$  and  $g$  evaluated at  $(\alpha_0, 0, 0)$ . Denote by  $L^*(\alpha_0)$ , the adjoint operator of  $L(\alpha_0)$ ,

$$L^*(\alpha_0) := \begin{pmatrix} A(\alpha_0) + d_1\partial^2/\partial x^2 & C(\alpha_0) \\ B(\alpha_0) & D(\alpha_0) + d_2\partial^2/\partial x^2 \end{pmatrix},$$

with the domain  $D_{L^*(\lambda_0)} = X_{\mathbf{C}}$ , and if  $(H_3)$  holds, then there exists  $q^* := (a_n^*, b_n^*)^T \cos(n/\ell)x \in X \oplus iX$  so that

$$L^*(\alpha_0)q^* = -i\omega_0q^*, \quad \langle q^*, q \rangle = 1 \quad \text{and} \quad \langle q^*, \bar{q} \rangle = 0.$$

Denote

$$\begin{cases} \tilde{q} = -[L(\alpha_0)]^{-1} \cdot [Q_{q\bar{q}} - \langle q^*, Q_{q\bar{q}} \rangle q - \langle \bar{q}^*, Q_{q\bar{q}} \rangle \bar{q}], \\ \hat{q} = (2i\omega_0I - L(\alpha_0))^{-1} [Q_{qq} - \langle q^*, Q_{qq} \rangle q - \langle \bar{q}^*, Q_{qq} \rangle \bar{q}], \end{cases}$$

then by [26],

$$c_1(\alpha_0) = \frac{i}{2\omega_0} \langle q^*, Q_{qq} \rangle \cdot \langle q^*, Q_{q\bar{q}} \rangle + \langle q^*, Q_{\bar{q},q} \rangle + \frac{1}{2} \langle q^*, Q_{\bar{q},\bar{q}} \rangle + \frac{1}{2} \langle q^*, C_{q,q,\bar{q}} \rangle.$$

With these notations, from [26], we have the following Hopf bifurcation theorem for the general reaction-diffusion system (5.1).

**Lemma 5.1** (Hopf bifurcation theorem). *Suppose  $(H_3)$  is satisfied. Then system (5.1) possesses a family of real-valued  $T(s)$ -periodic solutions  $(\alpha(s), u(s)(x, t), v(s)(x, t))$ , for  $s$  sufficiently small, bifurcating from  $(\alpha_0, 0, 0)$  at  $\alpha = \alpha_0$  in the space  $\mathbf{R} \times X$ , with  $\alpha(s), T(s) \in C^{k+1}$ . More precisely, there exists a unique  $n \in \mathbf{N}_0$  such that  $(u(s)(x, t), v(s)(x, t))$  can be parameterized in the following form:*

$$\begin{cases} \alpha(s) = \alpha_0 + \sum_{i=1}^{[k/2]} \mu_{2i} s^{2i} + o(s^{k+1}), \\ u(s)(x, t) = s(a_n e^{2\pi i t/T(s)} + \bar{a}_n e^{-2\pi i t/T(s)}) \cos \frac{n}{\ell} x + o(s^2), \\ v(s)(x, t) = s(b_n e^{2\pi i t/T(s)} + \bar{b}_n e^{-2\pi i t/T(s)}) \cos \frac{n}{\ell} x + o(s^2), \end{cases}$$

where

$$\begin{cases} T(s) = \frac{2\pi}{\omega_0} [1 + \sum_{j=1}^{[k/2]} \tau_{2j} s^{2j}] + o(s^{k+1}), \\ T''(0) = \frac{4\pi}{\omega_0} \tau_2 = -\frac{4\pi}{\omega_0^2} (\text{Im}(c_1(\alpha_0)) - \text{Re}(c_1(\alpha_0))\omega'(\alpha_0)/\gamma'(\alpha_0)), \end{cases}$$

and  $(a_n, b_n)$  is the eigenvector defined by

$$L_n(\alpha_0)(a_n, b_n)^T = i\omega_0(a_n, b_n)^T.$$

Here the coefficients  $\mu_{2i}$  and  $\tau_{2i}$  can be calculated according to [4]. In particular,  $\tau_2 = -(1/\omega_0)(\text{Im}(c_1(\alpha_0)) - \text{Re}(c_1(\alpha_0))\omega'(\alpha_0)/\gamma'(\alpha_0))$ . Moreover,

1. The bifurcation is supercritical, respectively subcritical, if

$$\frac{1}{\gamma'(\alpha_0)} \text{Re}(c_1(\alpha_0)) < 0 \quad (\text{respectively, } > 0)$$

2. If, in addition, all other eigenvalues of  $L(\alpha_0)$  have negative real parts, then the bifurcating periodic solutions are stable, respectively unstable, if  $\text{Re}(c_1(\alpha_0)) < 0$ , respectively  $> 0$ .

Next, we consider the steady state bifurcation for equation (5.2). We assume that, for some  $\alpha_0 \in \mathbf{R}$ , the following condition holds:

( $H_4$ ) There exists a neighborhood  $O$  of  $\alpha_0$  such that, for  $\alpha \in O$ ,  $L(\alpha)$  has a simple real eigenvalue  $\gamma(\alpha)$ , continuously differentiable in  $\alpha$ , with  $\gamma(\alpha_0) = 0$  and  $\gamma'(\alpha_0) \neq 0$ ; all other eigenvalues of  $L(\alpha)$  have non-zero real parts for  $\alpha \in O$ .

The following global bifurcation theorem is recalled from [26], and it is an application of a more general result in [16].

**Lemma 5.2** (Steady state bifurcation theorem). *Let  $I$  be a close interval which contains  $\alpha_0 \in \mathbf{R}$ . Suppose that ( $H_4$ ) is satisfied at  $\alpha = \alpha_0$ . Then there is a smooth curve  $\Gamma$  of solutions to (5.2) bifurcating from  $(\alpha_0, 0, 0)$ , and  $\Gamma$  is contained in a connected component  $\mathcal{C}$  of the set of nonzero solutions of (5.2); either  $\mathcal{C}$  is unbounded in  $I \times X$ , or  $\mathcal{C} \cap (\partial I \times X) \neq \emptyset$ , or  $\mathcal{C}$  contains a further bifurcation point  $(\alpha_*, 0, 0)$  with  $\alpha_* \neq \alpha_0$  such that 0 is an eigenvalue of  $L(\alpha_*)$ . More precisely, near  $(\alpha_0, 0, 0)$ ,  $\Gamma$  can be expressed as:  $\Gamma = \{(\alpha(s), u(s), v(s)) : s \in (-\varepsilon, \varepsilon)\}$ , where*

$$\begin{aligned}
 u(s) &= \mathbf{sa}_n \cos(nx/\ell) + s\psi_1(s), \\
 v(s) &= \mathbf{sb}_n \cos(nx/\ell) + s\psi_2(s), \\
 s &\in (-\varepsilon, \varepsilon)
 \end{aligned}
 \tag{5.3}$$

and  $\alpha : (-\varepsilon, \varepsilon) \rightarrow \mathbf{R}$ ,  $\psi_1, \psi_2 : (-\varepsilon, \varepsilon) \rightarrow Z$  are  $C^{k+1}$  functions, such that  $\alpha(0) = \alpha_0$ ,  $\psi_1(0) = \psi_2(0) = 0$ . Here,

1.  $Z = Z_1 \times Z_1$ , with  $Z_1 = \{u \in L^2(0, \ell\pi) : \int_0^{\ell\pi} u(x) \cos(nx/\ell) dx = 0\}$ ;
2. In (5.3),  $\mathbf{a}_n$  and  $\mathbf{b}_n$  satisfy:  $L(\alpha_0)[(\mathbf{a}_n, \mathbf{b}_n)^T \cos(nx/\ell)] = 0$ , for some  $n \in \mathbf{N} \cup \{0\}$ .

The following lemma presents an algorithm to determine the bifurcation direction of the steady state bifurcations of (5.2). This appears to be of independent interest.



**Lemma 5.3.** *Suppose that the conditions in Lemma 5.2 hold. Then the steady state bifurcations are always pitchfork bifurcations, that is,  $\alpha'(0) = 0$ ; the bifurcations are supercritical bifurcations if  $\alpha''(0) > 0$  and subcritical bifurcations if  $\alpha''(0) < 0$ , where  $\alpha''(0)$  is given by (5.5) below.*

*Proof.* By  $(H_4)$ , we can assume that  $q = (\mathbf{a}_n, \mathbf{b}_n)^T \cos(n/\ell)x$  with  $\mathbf{a}_n, \mathbf{b}_n \in \mathbf{R}$  satisfying  $L(\alpha_0)q = 0$ . We define  $F : \mathbf{R} \times X \rightarrow Y$  by

$$F(\alpha, u, v) := (d_1 u_{xx} + f(\alpha, u, v), d_2 v_{xx} + g(\alpha, u, v))^T.$$

By [15], it follows that

$$\alpha'(0) = -\frac{\langle l, F_{(u,v),(u,v)}[q, q] \rangle}{2\langle l, F_{\alpha(u,v)}[q] \rangle},$$

where,  $l \in Y^*(= Y)$  satisfying  $N(l) = R(L(\alpha_0))$ . The functional  $l$  here is given by  $\langle l, (p_1, p_2) \rangle = \int_0^{\ell\pi} (d_1^{-1} \mathbf{a}_n^* p_1(x) + d_2^{-1} \mathbf{b}_n^* p_2(x)) \cos(nx/\ell) dx$ , where  $(p_1, p_2) \in Y$ , and  $(\mathbf{a}_n^*, \mathbf{b}_n^*)$  is an eigenvector of  $L_n^*(\alpha_0)$ , the adjoint matrix of  $L_n(\alpha_0)$ . Notice that, for  $n \in \mathbf{N} \cup \{0\}$ ,  $L^*(\alpha_0)[(\mathbf{a}_n^*, \mathbf{b}_n^*)^T \cos(nx/\ell)] = 0$ , we have,

$$\langle l, F_{(u,v),(u,v)}[q, q] \rangle = \int_0^{\ell\pi} F_{(u,v),(u,v)}[q, q] \cdot p dx,$$

where  $p = (d_1^{-1} \mathbf{a}_n^*, d_2^{-1} \mathbf{b}_n^*) \cos(nx/\ell)$ . Then,

$$\alpha'(0) = -\frac{\int_0^{\ell\pi} F_{(u,v),(u,v)}[q, q] \cdot p dx}{2 \int_0^{\ell\pi} F_{\alpha(u,v)}[q] \cdot p dx}.$$

From direct calculations, it follows that

$$\begin{aligned} \int_0^{\ell\pi} F_{(u,v),(u,v)}[q, q] \cdot p dx &= \int_0^{\ell\pi} k_n \cos^3(nx/\ell) dx, \\ \int_0^{\ell\pi} F_{\alpha(u,v)}[q] \cdot p dx &= \int_0^{\ell\pi} r_n \cos^2(nx/\ell) dx, \end{aligned}$$

where

$$\begin{aligned} k_n &= d_1^{-1} \mathbf{a}_n^* (f_{uu} \mathbf{a}_n^2 + 2f_{uv} \mathbf{a}_n \mathbf{b}_n + f_{vv} \mathbf{b}_n^2 \\ &\quad + d_2^{-1} \mathbf{b}_n^* (g_{uu} \mathbf{a}_n^2 + 2g_{uv} \mathbf{a}_n \mathbf{b}_n + g_{vv} \mathbf{b}_n^2), \\ r_n &= d_1^{-1} \mathbf{a}_n^* (f_{\alpha u} \mathbf{a}_n + f_{\alpha v} \mathbf{b}_n) + d_2^{-1} \mathbf{b}_n^* (g_{\alpha u} \mathbf{a}_n + g_{\alpha v} \mathbf{b}_n), \end{aligned}$$

with all the partial derivatives of  $f$  and  $g$  evaluated at  $(\alpha_0, 0, 0)$ . Thus,

$$\alpha'(0) = -\frac{k_n \int_0^{\ell\pi} \cos^3(nx/\ell) dx}{2r_n \int_0^{\ell\pi} \cos^2(nx/\ell) dx} = 0,$$

since, for  $n \in \mathbf{N}$ ,  $\int_0^{\ell\pi} \cos^3(nx/\ell) dx = 0$ . Hence, the bifurcation is pitchfork bifurcation. To determine the bifurcation direction, we need to calculate  $\alpha''(0)$ , which, according to [15], is given by

$$\begin{aligned} \alpha''(0) &= -\frac{\langle l, F_{(u,v),(u,v),(u,v)}[q, q, q] \rangle + 3\langle l, F_{(u,v),(u,v)}[q, \theta] \rangle}{3\langle l, F_{\alpha(u,v)}[q] \rangle} \\ &= -\frac{\int_0^{\ell\pi} F_{(u,v),(u,v),(u,v)}[q, q, q] \cdot p dx}{3 \int_0^{\ell\pi} F_{\alpha(u,v)}[q] \cdot p dx} \\ &\quad + \frac{3 \int_0^{\ell\pi} F_{(u,v),(u,v)}[q, \theta] \cdot p dx}{3 \int_0^{\ell\pi} F_{\alpha(u,v)}[q] \cdot p dx} \end{aligned}$$

where  $\theta \in Z$  uniquely solves the following equation:

$$(5.4) \quad F_{(u,v),(u,v)}[q, q] + F_{(u,v)}[\theta] = 0.$$

Direct computation implies that

$$\begin{aligned} &F_{(u,v),(u,v),(u,v)}[q, q, q] \\ &= \left( f_{uuu} \mathbf{a}_n^3 + 3f_{uuv} \mathbf{b}_n \mathbf{a}_n^2 + 3f_{uvv} \mathbf{b}_n^2 \mathbf{a}_n + f_{vvv} \mathbf{b}_n^3 \right) \cos^3(nx/\ell) \\ &\quad + \left( g_{uuu} \mathbf{a}_n^3 + 3g_{uuv} \mathbf{b}_n \mathbf{a}_n^2 + 3g_{uvv} \mathbf{b}_n^2 \mathbf{a}_n + g_{vvv} \mathbf{b}_n^3 \right) \end{aligned}$$

Then  $\int_0^{\ell\pi} F_{(u,v),(u,v),(u,v)}[q, q, q] \cdot p dx = s_n \int_0^{\ell\pi} \cos^4(nx/\ell) dx$ , where

$$\begin{aligned} s_n &= d_1^{-1} \mathbf{a}_n^* (f_{uuu} \mathbf{a}_n^3 + 3f_{uuv} \mathbf{b}_n \mathbf{a}_n^2 + 3f_{uvv} \mathbf{b}_n^2 \mathbf{a}_n + f_{vvv} \mathbf{b}_n^3), \\ &\quad + d_2^{-1} \mathbf{b}_n^* (g_{uuu} \mathbf{a}_n^3 + 3g_{uuv} \mathbf{b}_n \mathbf{a}_n^2 + 3g_{uvv} \mathbf{b}_n^2 \mathbf{a}_n + g_{vvv} \mathbf{b}_n^3). \end{aligned}$$

Now we shall compute the value of  $\int_0^{\ell\pi} F_{(u,v),(u,v)}[q, \theta] \cdot p \, dx$ . To that end, we let

$$\theta = \sum_{m=0}^{\infty} \begin{pmatrix} \theta_m^1 \\ \theta_m^2 \end{pmatrix} \cos \frac{m}{\ell} x,$$

with the coefficients  $\theta_m^1$  and  $\theta_m^2$  to be determined later. Then (5.4) is equivalent to

$$\begin{aligned} & \begin{pmatrix} f_{uu} \mathbf{a}_n^2 + 2f_{uv} \mathbf{b}_n \mathbf{a}_n + f_{vv} \mathbf{b}_n^2 \\ g_{uu} \mathbf{a}_n^2 + 2g_{uv} \mathbf{b}_n \mathbf{a}_n + g_{vv} \mathbf{b}_n^2 \end{pmatrix} \cos^2(nx/\ell) \\ &= - \begin{pmatrix} f_u + d_1 \frac{\partial^2}{\partial x^2} & f_v \\ g_u & g_v + d_2 \frac{\partial^2}{\partial x^2} \end{pmatrix} \sum_{n=0}^{\infty} \begin{pmatrix} \theta_m^1 \\ \theta_m^2 \end{pmatrix} \cos \frac{m}{\ell} x. \end{aligned}$$

Thus, by comparing the coefficients of  $\cos(mx/\ell)$  with  $m \in \mathbf{N} \cup \{0\}$  in the equation, we obtain that

$$\begin{pmatrix} \theta_m^1 \\ \theta_m^2 \end{pmatrix} = \begin{pmatrix} 0 \\ 0 \end{pmatrix},$$

for all  $m \in \mathbf{N} \setminus \{2n\}$ ,

$$\begin{aligned} & \begin{pmatrix} \theta_0^1 \\ \theta_0^2 \end{pmatrix} \\ &= \frac{1}{2D_0} \begin{pmatrix} g_v(f_{uu} \mathbf{a}_n^2 + 2f_{uv} \mathbf{b}_n \mathbf{a}_n + f_{vv} \mathbf{b}_n^2) - f_v(g_{uu} \mathbf{b}_n^2 + 2g_{uv} \mathbf{b}_n \mathbf{a}_n + g_{vv} \mathbf{b}_n^2) \\ f_u(g_{uu} \mathbf{a}_n^2 + 2g_{uv} \mathbf{b}_n \mathbf{a}_n + g_{vv} \mathbf{b}_n^2) - g_u(f_{uu} \mathbf{b}_n^2 + 2f_{uv} \mathbf{b}_n \mathbf{a}_n + f_{vv} \mathbf{b}_n^2) \end{pmatrix}, \end{aligned}$$

and

$$\begin{aligned} & \begin{pmatrix} \theta_{2n}^1 \\ \theta_{2n}^2 \end{pmatrix} = \frac{1}{2D_{2n}} \\ & \times \begin{pmatrix} (g_v - \frac{4d_2 n^2}{\ell^2})(f_{uu} \mathbf{a}_n^2 + 2f_{uv} \mathbf{b}_n \mathbf{a}_n + f_{vv} \mathbf{b}_n^2) - f_v(g_{uu} \mathbf{a}_n^2 + 2g_{uv} \mathbf{b}_n \mathbf{a}_n + g_{vv} \mathbf{b}_n^2) \\ (f_u - \frac{4d_1 n^2}{\ell^2})(g_{uu} \mathbf{a}_n^2 + 2g_{uv} \mathbf{b}_n \mathbf{a}_n + g_{vv} \mathbf{b}_n^2) - g_u(f_{uu} \mathbf{a}_n^2 + 2f_{uv} \mathbf{b}_n \mathbf{a}_n + f_{vv} \mathbf{b}_n^2) \end{pmatrix}, \end{aligned}$$

where  $D_0$  and  $D_{2n}$  are the determinants of  $L_0$  and  $L_{2n}$ , respectively. Thus, we have,

$$\theta = \begin{pmatrix} \theta_{2n}^1 \\ \theta_{2n}^2 \end{pmatrix} \cos \frac{2n}{\ell} x + \begin{pmatrix} \theta_0^1 \\ \theta_0^2 \end{pmatrix},$$

or equivalently,

$$\theta = \begin{pmatrix} \Theta_n^1 \\ \Theta_n^2 \end{pmatrix} \cos^2 \frac{n}{\ell} x + \begin{pmatrix} \Theta_0^1 \\ \Theta_0^2 \end{pmatrix},$$

where

$$\Theta_n^1 = 2\theta_{2n}^1, \quad \Theta_n^2 = 2\theta_{2n}^2, \quad \Theta_0^1 = \theta_0^1 - \theta_{2n}^1, \quad \Theta_0^2 = \theta_0^2 - \theta_{2n}^2.$$

Direct calculations show that

$$\begin{aligned} & F_{(u,v),(u,v)}[q, \theta] \\ &= \begin{pmatrix} (f_{uu}\mathbf{a}_n + f_{uv}\mathbf{b}_n)\Theta_0^1 + (f_{uv}\mathbf{a}_n + f_{vv}\mathbf{b}_n)\Theta_0^2 \\ (g_{uu}\mathbf{a}_n + g_{uv}\mathbf{b}_n)\Theta_0^1 + (g_{uv}\mathbf{a}_n + g_{vv}\mathbf{b}_n)\Theta_0^2 \end{pmatrix} \cos(nx/\ell) \\ &+ \begin{pmatrix} (f_{uu}\mathbf{a}_n + f_{uv}\mathbf{b}_n)\Theta_n^1 + (f_{uv}\mathbf{a}_n + f_{vv}\mathbf{b}_n)\Theta_n^2 \\ (g_{uu}\mathbf{a}_n + g_{uv}\mathbf{b}_n)\Theta_n^1 + (g_{uv}\mathbf{a}_n + g_{vv}\mathbf{b}_n)\Theta_n^2 \end{pmatrix} \cos^3(nx/\ell), \end{aligned}$$

By

$$\int_0^{\ell\pi} \cos^2\left(\frac{nx}{\ell}\right) dx = \frac{\ell\pi}{2}$$

and

$$\int_0^{\ell\pi} \cos^4\left(\frac{nx}{\ell}\right) dx = \frac{3\ell\pi}{8},$$

we have

$$\int_0^{\ell\pi} F_{(u,v),(u,v)}[q, \theta] \cdot p dx = \frac{\ell\pi}{2} t_n^1 + \frac{3\ell\pi}{8} t_n^2,$$

where

$$\begin{aligned} t_n^1 &= d_1^{-1} \mathbf{a}_n^* [(f_{uu}\mathbf{a}_n + f_{uv}\mathbf{b}_n)\Theta_0^1 + (f_{uv}\mathbf{a}_n + f_{vv}\mathbf{b}_n)\Theta_0^2] \\ &+ d_2^{-1} \mathbf{b}_n^* [(g_{uu}\mathbf{a}_n + g_{uv}\mathbf{b}_n)\Theta_0^1 + (g_{uv}\mathbf{a}_n + g_{vv}\mathbf{b}_n)\Theta_0^2], \\ t_n^2 &= d_1^{-1} \mathbf{a}_n^* [(f_{uu}\mathbf{a}_n + f_{uv}\mathbf{b}_n)\Theta_n^1 + (f_{uv}\mathbf{a}_n + f_{vv}\mathbf{b}_n)\Theta_n^2] \\ &+ d_2^{-1} \mathbf{b}_n^* [(g_{uu}\mathbf{a}_n + g_{uv}\mathbf{b}_n)\Theta_n^1 + (g_{uv}\mathbf{a}_n + g_{vv}\mathbf{b}_n)\Theta_n^2], \end{aligned}$$

Therefore,

$$(5.5) \quad \alpha''(0) = -\frac{s_n + 4t_n^1 + 3t_n^2}{4r_n}.$$

This completes the proof of this lemma.  $\square$

## REFERENCES

1. P. De Kepper, V. Castets, E. Dulos and J. Boissonade, *Turing-type chemical patterns in the chlorite-iodide-malonic acid reaction*, Phys. D **49** (1991), 161–169.
2. I.R. Epstein and J.A. Pojman, *An introduction to nonlinear chemical dynamics*, Oxford University Press, Oxford, 1998.
3. P. Gray and S.K. Scott, *Chemical oscillations and instabilities*, Oxford Univ. Press, New York-Oxford, 1990.
4. B.D. Hassard, N.D. Kazarinoff and Y.-H. Wan, *Theory and application of Hopf bifurcation*, Cambridge University Press, Cambridge, 1981.
5. S. Hsu and J. Shi, *Relaxation oscillator profile of limit cycle in predator-prey system*, Disc. Cont. Dyn. Syst. **11** (2009), 893–911.
6. J. Jang, W. Ni and M. Tang, *Global bifurcation and structure of Turing patterns in the 1-D Lengyel-Epstein model*, J. Dyn. Diff. Eqs. **16** (2005), 297–320.
7. S.L. Judd and M. Silber, *Simple and superlattice Turing patterns in reaction-diffusion systems: Bifurcation, bistability, and parameter collapse*, Phys. D **136** (2000), 45–65.
8. I. Lengyel and I.R. Epstein, *A chemical approach to designing Turing patterns in reaction-diffusion system*, Proc. Natl. Acad. Sci. **89** (1992), 3977–3979.
9. ———, *Modeling of Turing structure in the Chlorite-iodide-malonic acid-starch reaction system*, Science **251** (1991), 650–652.
10. S.G. Lenhoff and H.M. Lenhoff, *Hydra and the birth of experimental biology-1744*, Boxwood, Pacific Grove, CA, 1986.
11. P.K. Maini, K.J. Painter and H.N.P. Chau, *Spatial pattern formation in chemical and biological systems*, Faraday Transactions **20** (1997), 3601–3610.
12. J.D. Murray, *Mathematical biology*, Third edition. I. *An introduction*, Interdisc. Appl. Math. **17**, Springer-Verlag, New York, 2002; II. *Spatial models and biomedical applications*, Interdisc. Appl. Math. **18**, Springer-Verlag, New York, 2003.
13. W. Ni and M. Tang, *Turing patterns in the Lengyel-Epstein system for the CIMA reaction*, Trans. Amer. Math. Soc. **357** (2005), 3953–3969.
14. Y. Nishiura, *Global structure of bifurcating solutions of some reaction-diffusion systems*, SIAM J. Math. Anal. **13** (1982), 555–593.
15. J. Shi, *Persistence and bifurcation of degenerate solutions*, J. Funct. Anal. **169** (1999), 494–531.
16. J. Shi and X. Wang, *On global bifurcation for quasilinear elliptic systems on bounded domains*, J. Diff. Equat. **246** (2009), 2788–2812.

17. L.E. Stephenson and D.J. Wollkind, *Weakly nonlinear stability analyses of one-dimensional Turing pattern formation in activator-inhibitor/immobilizer model systems*, J. Math. Biol. **33** (1995), 771–815.
18. I. Takagi, *Point-condensation for a reaction-diffusion system*, J. Diff. Equat. **61** (1986), 208–249.
19. A. Trembley, *Mémoires, Pour Servir à l'Histoire d'un Genre de Polypes d'Eau Douce, à Bras en Forme de Cornes*, Verbeek, Leiden, The Netherlands, 1744.
20. A. Turing, *The chemical basis of morphogenesis*, Philos. Trans. Roy. Soc. Lond. **237** (1952), 37–72.
21. D.J. Wollkind and L.E. Stephenson, *Chemical Turing pattern formation analyses: Comparison of theory with experiment*, SIAM J. Appl. Math. **61** (2000), 387–431.
22. J. Wu, *Theory and applications of partial functional-differential equations*, Appl. Math. Sci. **119**, Springer-Verlag, New York, 1996.
23. ———, *Symmetric functional differential equations and neural networks with memory*, Trans. Amer. Math. Soc. **350** (1998), 4799–4838.
24. F. Yi, J. Wei and J. Shi, *Diffusion-driven instability and bifurcation in the Lengyel-Epstein model*, Nonl. Anal. Real World Appl. **9** (2008), 1038–1051.
25. ———, *Global asymptotical behavior of the Lengyel-Epstein reaction-diffusion system*, Appl. Math. Lett. **22** (2009), 52–55.
26. ———, *Bifurcation and spatio-temporal patterns in a diffusive homogenous predator-prey system*, J. Diff. Equat. **246** (2009), 1944–1977.

DEPARTMENT OF MATHEMATICS, MICHIGAN STATE UNIVERSITY, EAST LANSING, MI 48824

**Email address:** hit\_jjy1986@hotmail.com

Y.Y. TSENG FUNCTIONAL ANALYSIS RESEARCH CENTER, HARBIN NORMAL UNIVERSITY, HARBIN, HEILONGJIANG, 150025, P.R. CHINA AND DEPARTMENT OF MATHEMATICS, COLLEGE OF WILLIAM AND MARY, WILLIAMSBURG, VIRGINIA, 23187

**Email address:** shij@math.wm.edu

DEPARTMENT OF MATHEMATICS, HARBIN INSTITUTE OF TECHNOLOGY, HARBIN, HEILONGJIANG, 150001, P.R. CHINA

**Email address:** weijj@hit.edu.cn

DEPARTMENT OF APPLIED MATHEMATICS, HARBIN ENGINEERING UNIVERSITY, HARBIN, HEILONGJIANG, 150001, P.R. CHINA AND MATHEMATICS SCHOOL AND INSTITUTE, JILIN UNIVERSITY, CHANGCHUN, JILIN, 130012, P.R. CHINA

**Email address:** fengqi.yi@gmail.com